IN-36-CR

234681

p-52

FINAL REPORT

SUBMITTED TO: National Aeronautics and Space Administration, Langley Research Center, Hampton, Virginia 23665

INSTITUTION: Department of Physics, Hampton University, Hampton, Virginia 23668

TITLE OF RESEARCH: Development of Mid-Infrared Solid State Lasers for Spaceborne Lidar

NASA GRANT NUMBER: NAG-1-877

PERIOD COVERED BY THIS REPORT: April 13, 1988 - October 15, 1989

PRINCIPAL INVESTIGATOR: Donald A. Whitney

CO-PRINCIPAL INVESTIGATOR: Kyong H. Kim

(NASA-CR-183290) DEVELOPMENT OF MID-INFRARED SOLID STATE LASERS FOR SPACEBORNE LIDAR Final Report, 13 Apr. 1988 - 15 Oct. 1989 (Hampton Inst.) 52 p

N90-13772

CSCL 20E G3/36

Unclas 0234681

CONTENTS

Summary

This report covers work performed during the period from March 1, 1988 to October 15, 1989 under NASA grant number NAG-1-877 entitled "Development of mid-infrared solid state lasers for spaceborne lidar". During this period we have investigated laser performance of Ho^{3+}:Tm^{3+}:Cr^{3+}:YAG crystals under both Cr:GSAG laser and flashlamp pumping. A flashlamp pumped Cr:GSAG laser was built to simulate high power quasi-cw laser diode pumping of a 2.1 μm holmium laser. The 2.1 μm output laser energy exceeded more than 14 mJ, the highest value reported to date under laser pumping near 785 nm. This was obtained in a pulse length of nearly 650 μs from a 3 x 3 mm Ho:Tm:Cr:YAG rod by using the flashlamp-pumped Cr:GSAG laser as a pumping source at the diode laser wavelength, 785 μm. In addition, Ho:Tm:Cr:YAG crystals with various Tm^{3+} concentrations have been evaluated for flashlamp-pumped normal mode and Q-switched 2.1 μm laser operations under a wide variety of experimental conditions in order to understand internal dynamic processes among the ions and to determine an optimum lasing condition. An increase of the laser slope efficiency was observed with the increase of the Tm^{3+} concentration from 2.5 atomic % to 4.5 atomic %. The thermal dependence of the laser performance was also investigated. Q-switched laser output energies corresponding to nearly 100 % of the normal-mode laser energies were obtained in a strong single spike of 200 ns pulse length by optimizing the opening time of a lithium niobate Q-switch.

Investigation of 2.1 μm Holmium Lasers Under Flashlamp and Laser Pumpings

Development of solid state lasers with Ho^{3+}, Tm^{3+} and/or Er^{3+} doped crystals have been pursued by NASA for eye-safe mid-infrared LIDAR, light detection and ranging, applications. As a part of the project we have been working on evaluation of the Ho^{3+}:Tm^{3+}:Cr^{3+}:YAG laser systems under both flashlamp and laser-diode simulator pumpings. A flashlamp pumped Cr:GSAG laser was used as a simulator of high power quasi-cw laser diodes pumping a 2.1 μm holmium laser. Cr:GSAG laser pulses of 1-ms pulse length and more than 200 mJ energy were obtained in the wavelength range of 780 to 787 nm which overlaps the absorption spectrum of Tm^{3+} ions in a Ho:Tm:Cr:YAG crystal. The detailed design of the pulse forming network and system design can be found in Refs. 1 and 2. For the space-based LIDAR systems the system efficiency, lifetime and reliability are major considerations. Thus, the laser-diode pumped laser systems will be an ultimate system for that application. However, the technology for the high power laser diode is still under development. The Cr:GSAG laser is an alternative pumping source to study the 2.1 μm laser system with high power laser pumping at the diode laser wavelength. In our research the flashlamp-pumped Cr:GSAG laser played an important role in providing high pump powers at the diode laser wavelength to 2.1 μm Ho^{3+}:Tm^{3+}:YAG laser systems. The 2.1 μm output laser energy, which exceeded more than 14 mJ, the highest value reported to date under laser pumping near 785 nm, was obtained in a pulse length of nearly 650 μs from a Ho:Tm:Cr:YAG crystal by using a flashlamp-pumped Cr:GSAG laser as a pumping source at 785 μm. The highest quasi-cw 2.1 μm laser power, as obtained by dividing the laser energy values by the corresponding pulse length, was approximately 22 W at the Cr:GSAG input laser power of 137 W. The slope efficiency with a 98 % reflective output mirror was about 17.6 % which corresponds to 33.0 % slope efficiency in terms of the absorbed input power while those with a 95 % reflective mirror are

16.5 % and 30.9 %, respectively. The detailed laser performance is described in a draft prepared for publication attached in Appendix I.

Even though diode-pumped solid-state lasers are ultimate systems for space-borne lidar application, the flashlamp pumped laser systems still have several practical advantages over the diode-pumped lasers. The major advantage is that the flashlamp systems are well developed and easily accessible. Especially in high laser energy (or power) applications, the technology for the flashlamp pumped laser system is well developed compared to that for the diode lasers and is capable of delivering a high laser energy (or power) at a relatively low cost. Especially, in recent years the efficiency of flashlamp pumped laser systems has been improved greatly by codoping Cr^{3+}-ions in rare earth ion doped crystals and utilizing its broad absorption spectrum over the flashlamp emission. Thus, close investigation of the 2.1 μm rare earth laser systems including understanding of the mechanisms of the energy transfer processes between the chromium ions and rare earth ions such as Tm^{3+}, Ho^{3+} and Er^{3+} is very important to obtain an efficient flashlamp-pumped 2.1 μm laser system. The main concern of this research was focused on determination of optimum Tm^{3+} concentration in Ho^{3+}:Tm^{3+}:Cr^{3+}:YAG crystals for efficient Q-switched laser output by studying laser performance of the Ho^{3+}:Tm^{3+}:Cr^{3+}:YAG crystals with different Tm^{3+} concentrations at relatively fixed Ho^{3+} and Cr^{3+} concentrations. Coherent Laser Technology provided three Ho^{3+}:Tm^{3+}:Cr^{3+}:YAG crystals, each with a Tm^{3+} concentration of 2.5, 3.5 and 4.5 atomic %, respectively, and with the same 0.45 at. % Ho^{3+} and 1.5 at. % Cr^{3+} concentrations. Laser output parameters of these three laser rods, such as energy, slope efficiency, thresholds, pulse length and wavelength, were determined as a function of operating temperature, Tm^{3+} concentration, output mirror reflectivity, input electrical energy and Q-switch opening time. An increase of the laser slope efficiency was observed with the increase of the Tm^{3+} concentration from 2.5 atomic % to 4.5 atomic %. Two laser transitions at 2.098 and 2.091 μm were observed and the possible origin of the 2.091 μm laser transition was identified in this measurement. Q-switched laser output energies corresponding to about 100 % of the normal-mode laser energies were obtained in a strong single spike of pulse length of around 200 ns by optimizing the opening time of a lithium niobate Q-switch. The detailed experimental results are described in the draft prepared for publication in Appendix II.

In addition to the Contractor Reports referenced, preliminary results have been published and presented in References 3-4.

References

1. Donald A. Whitney and Kyong H.Kim, "Development of Mid-Infrared Solid-State Lasers for Spaceborne Lidar," NASA Contractor Report, NASA-CR-183341, 32 pp., October 1988.

2. Donald A. Whitney and Kyong H.Kim, "Development of Mid-Infrared Solid-State Lasers for Spaceborne Lidar," NASA Contractor Report, NASA-CR-185012, April 1989.

3. Young S. Choi, Kyong H. Kim, Donald A. Whitney, Robert V. Hess, Norman P. Barnes, Clayton H. Bair and Philip Brockman, "Development of Flashlamp-Pumped Q-Switched Ho:Tm:Cr:YAG Lasers for Mid-Infrared Lidar Application," Proceedings of the 1989 NASA HBCU Forum, Huntsville, AL, March 1989.

4. Kyong H. Kim, Young S. Choi, Donald A. Whitney, Norman P. Barnes, Robert V. Hess, Clayton H. Bair and Philip Brockman, "Development of a Ho:Tm:Cr:YAG Laser for Mid-Infrared Lidar Application," The Virginia Journal of Science, **Vol. 40 (2)**, p. 53, 1989.

APPENDIX I and II

Drafts prepared for publication

Study of a 2.1 μm holmium laser under high power laser pumping at 785 nm

Kyong H. Kim, Young S. Choi

Department of Physics, Hampton University, Hampton, Virginia 23668

Robert V. Hess, Clayton H. Bair, Philip Brockman, Norman P. Barnes

NASA Langley Research Center, Hampton, Virginia 23665

George W. Henderson

Department of Physics, Virginia State University, Petersburg, Virginia 23803

Abstract

The 2.1 μm output laser energy exceeding more than 14 mJ, the highest value reported to date under laser pumping at near 785 nm, was obtained in a pulse length near 650 μs from a Ho:Tm:Cr:YAG crystal by using a flashlamp-pumped Cr:GSAG laser as a pumping source at 785 μm. The flashlamp pumped Cr:GSAG laser was built to simulate a high power quasi-cw laser diode pumping a 2.1 μm holmium laser. Cr:GSAG laser pulses of 1-ms long and of energy of more than 200 mJ were obtained at a wavelength range of 780 to 787 nm which overlaps with the absorption spectrum of Tm^{3+} ions in a Ho:Tm:Cr:YAG crystal. Slope efficiency of 33 % in terms of absorbed input energy was obtained from the Cr:GSAG laser pumped 2.1 μm holmium laser with a 3 x 3 mm Ho:Tm:Cr:YAG rod and with a 98 % output mirror at room temperature.

In recent years there has been a significant interest among laser science community in developing laser-diode-pumped 2.1 μm holmium lasers for eye-safe LIDAR (light detection and ranging) applications in remote sensing of wind velocity and atmospheric constituents such as CO_2 and H_2O. Laser- diode-pumped lasers provide relatively high efficiency, long lifetime, reliability and simplicity compared to flashlamp-pumped lasers or gas or liquid lasers. The technology on the laser-diode-pumped solid-state lasers has been improved significantly along with the rapid progress in high power laser diode development during the last several years.[1] Especially, the 2.1 μm holmium laser has been recognized as a prospective candidate for an efficient laser under diode pumping by utilizing the energy transfer from the Tm^{3+} ions in the Ho^{3+} and Tm^{3+} codoped crystals where Tm^{3+} ions absorb the diode laser energy and enhance the quantum efficiency through internal cross-relaxation processes. Progress on laser-diode-pumped 2.1 μm lasers has been reported recently in several papers.[2-7]

However, the power level of the laser diodes is still too low to achieve a reasonable 2.1 μm laser for the LIDAR application and their prices are very high. So far demonstration of the laser-diode-pumped 2.1 μm lasers has been limited to a low power level. In order to predetermine the laser performance of the holmium crystals at 2.1 μm when they are pumped by high power laser diodes, we have developed a flashlamp pumped Cr^{3+}:CSAG (chromium doped gadolinium scandium aluminum garnet) laser as a high power laser diode simulator. Flashlamp pumped Cr:CSAG lasers were demonstrated by several groups previously and recognized as a tunable laser in a wavelength range of 765 to 801 nm.[8,9] Recently other lasers such as alexandrite and dye lasers were employed to pump the 2.1 μm lasers at near 785 nm, but the 2.1 μm laser output energy (and power) was low.[10,11] Here we report achievement of long-pulsed high pump energies at a wavelength range of 780-787 nm from the Cr:CSAG laser and of a 2.1 μm laser output from the holmium laser which is a factor of 10^2 to 10^3 higher than any other reported value.

Fig. 1 shows the schematic diagram of experimental setup used. A xenon flashlamp with 4 mm bore diameter and 7.62 cm long arc length was used to pump the Cr:GSAG laser, and a three LC section pulse-forming-network with each L = 186 μH and C = 150 μF was employed to get critically damped 1-ms long discharge pulses at a 300 J input energy. The pulses were of a square-shape with rise time and fall time of about 160 μs, respectively. The pulse shape stayed relatively constant as the input electrical energy was changed. This long pulse length was designed to utilize the long upper state lifetime of Ho^{3+} ions at room temperature which is typically 8 ms. The Cr^{3+} concentration of the Cr:GSAG laser rod was 1.0 atomic % and its size was 5 mm in diameter and 80 mm in length. The flashlamp and laser rod were surrounded by separate flow tubes. In order to avoid the uv light induced color center or other solarization effect, a uranium doped flow tube was used around the flashlamp and a $K_2CrO_4 + H_2O$ solution of 0.01 M concentration was circulated in both flow tubes forming about 2.5 mm and 1 mm thickness around the flashlamp and laser rod, respectively. The pumping cavity was of a simple single elliptical shape made of a piece of aluminum foil and a brass tube of 35.5 mm major diameter and 34.0 mm minor diameter. The resonator consisted of a highly reflective mirror and a 95 % reflective mirror at 790 nm. Both mirrors had a radius of curvature of 1.0 m. The resonator length was about 78 cm. Typical laser output energy versus the electrical input energy is shown in Fig. 2. The laser output energy was increasing linearly with the input energy above 170 J, but no attempt has been made to achieve more than 200 mJ of output energy to avoid possible optical damage. Even though the pump light below 450 nm was blocked with the K_2CrO_4 solution, degradation of the laser output energy was observed in consecutive operations as shown in the figure. There were about 50 shots between runs in Fig. 2. At the beginning of this research the Cr:GSAG laser output was low and was degrading gradually. After annealing the laser rod in an oven at 150 °C for 1 hour, the laser output energy was increased by a factor of apparently 2. Even though the Cr:GSAG laser kept degrading after the annealing process, the degrading process was slow enough so that it could be used as a high power laser diode simulator for the 2.1 μm laser pumping. It could deliver more than 100 mJ over one month at daily uses.

The spectrum of the Cr:GSAG laser was measured with an optical multichannel analyzer and is compared in Fig. 3 with the absorption spectrum of the Ho(0.36 atomic %):Tm(5.90 at. %):Cr(0.85 at. %):YAG used for the 2.1 μm laser operation. Even without any tuning element in the resonator the free running laser wavelength was observed in the region of 780 to 787 nm which overlaps the absorption peak of the Tm^{3+} ions in the Ho:Tm:Cr:YAG crystal.

The Cr:GSAG laser beam was focused with a lens of focal length of 80 mm on the Ho:Tm:Cr:YAG laser rod through a highly reflective at 2.1 μm and highly transmissive at 0.79 μm mirror which has a radius of curvature of 10 cm. The pump beam spot size on the holmium rod was about 0.54 mm in radius. In order to increase the mode volume and to obtain a proper mode matching between the pump laser beam and the 2.1 μm laser beam, the Ho:Tm:Cr:YAG rod was placed about 5 mm apart from the highly reflective end mirror as shown in Fig. 1. The output mirror also has a radius of curvature of 10 cm and the 2.1 μm laser cavity length was about 17.5 cm. The size of the Ho:Tm:Cr:YAG rod was 3 mm in diameter and 3 mm in length, and both ends were anti-reflection coated at 2.1 μm. A cut-off filter below 850 nm was placed in front of the detector to block the Cr:GSAG pump laser beam as shown in Fig.1 and the 2.1 μm laser output energy was calibrated according to the transmittance of the filter at the 2.1 μm which was about 89 %. The detector was a pyroelectric energy meter for energy measurement and a liquid-nitrogen-cooled HgCdTe detector for pulse shape measurement.

Fig. 4 shows the measured 2.1 μm laser output energies with 98 % and 95 % reflective output mirrors as a function of the absorbed Cr:GSAG pump laser energy. The optimum output coupling was observed with the 98 % reflective mirror. The highest 2.1 μm laser energy obtained was 14 mJ, the highest number ever reported with laser pumping near 800 nm, at the input energy of 89 mJ. The corresponding slope efficiency was 33.6 % while the slope efficiency obtained with the 95 % was 26.3 %. The absorbed pump laser energy corresponds approximately 53 % of the pump laser energy before the focusing lens when Fresnel loss and reabsorption by rod surface reflections were taken into account in the measured values of the pump beam transmission through the laser rod. The slope efficiencies correspond to 17.9 % and 14.0 % in terms of the incoming Cr:GSAG laser energy for the 98 % and 95 %

reflective mirrors, respectively. Since the Cr:GSAG laser output energy was degrading slightly, the pump laser energies were measured before and after the 2.1 μm laser energy measurement and their average values were taken to obtain relatively accurate values. Even though our system can deliver more than 14 mJ of the 2.1 μm laser output energy, no attempt was made at the Cr:GSAG pump laser energy of above 115 mJ to avoid any possible optical damage.

The typical pulse shapes are shown in Fig. 5. In Fig. 5(a) the top trace shows the square-shaped flashlamp pulse and the middle trace shows the Cr:GSAG laser pulse while the bottom trace shows the 2.1 μm laser pulse. Figs. 5(b) and 5(c) show the details of the beginning of the two laser pulses. Both pulses are of a continuous wave nature with spikes on the top, and especially the 2.1 μm laser pulses show an apparent relaxation oscillation at the beginning. Fig. 6 shows the summary of the delay of 2.1 μm laser appearance with respect to the beginning of the Cr:GSAG laser pulse and the length of the 2.1 μm laser pulses as a function of the absorbed pump laser energy. The 2.1 μm laser pulse length depends on the pulse length of the Cr:GSAG laser which also depends on the electrical input energy. By dividing the laser energy values by the corresponding pulse length, the average (or quasi-cw) powers within the pulses were obtained and plotted in Fig. 7. The highest quasi-cw 2.1 μm laser power was approximately 22 W at the Cr:GSAG input laser power of 137 W. The corresponding slope efficiency for the 98 % reflective mirror is about 17.6 % which also corresponds to 33.0 % slope efficiency in terms of the absorbed input power while those for the 95 % reflective mirror are 16.5 % and 30.9 %, respectively.

The 2.1 μm laser output measurements were performed on the basis of single shot, less than one pulse per minute, because immediate shots following another shot delivered lower 2.1 μm laser output energies. The cooling mechanisms connected to the laser rod were conductive cooling by an aluminum holder through the side surface of the rod and convectional cooling by the air on the rod ends. The low laser output energies observed in the immediately following shots after one shot may possibly be attributed to thermal population in lower laser level caused by the slow cooling processes.

The decrease of the slope efficiency of the 2.1 μm lasers with low reflective output mirrors agrees with results obtained with others[11,12] and can be explained with the upconversion loss from the upper laser level of the Ho^{3+} ions. From our preliminary theoretical analysis we could show the tendency of decreasing slope efficiency by introducing the upconversion loss in the rate equation model. However, more accurate analysis can be done with close investigation of the dynamic processes among the Ho^{3+} and Tm^{3+} ions in the laser crystal.

A Q-switched laser output of 0.5 mJ with a pulse width of 0.7 μs was also obtained with a mechanical chopper. Fig. 8 shows the comparison of the Q-switched laser output with the normal-mode laser output measured with a 95 % reflective output mirror when the optical alignment is not the best. The Q-switched slope efficiency is about 1.0 % while the normal-mode slope efficiency is 27.2 %. This low Q-switched slope efficiency may be attributed to the loss caused by the upconversion processes in the Ho^{3+}-ions and slow Q-switch opening. The risetime of the chopper opening was about 30 μs which is very long compared to the Q-switched pulse length. The chopper's opening time was delayed about 200 μs after the pump laser beam ended in order to obtain the single Q-switched spike. Fig. 9(a) shows the chopper opening time compared to the flashlamp and Cr:GSAG laser pulses for a single Q-switched spike at the electrical input energy of 245 J which delivers about 68 mJ of the Cr:GSAG laser energy. Fig. 9(b) shows the pulse shape of the typical Q-switched single spike. Multiple Q-switched spikes were observed with Q-switch openings of earlier than the 200 μs delay. This mutiple spike phenomenon is related to the energy transfer process from Tm^{3+} to Ho^{3+} ions and the relatively long upper state lifetime. A fast Q-switched experiment is being planned in our laboratory to determine the possibility of improvement of the Q-switched laser efficiency because in our research on flashlamp-pumped Ho^{3+}:Tm^{3+}:Cr^{3+}:YAG lasers Q-switched laser output energies corresponding to about 100 % of the normal-mode laser energies were observed.[13]

In conclusion, we can conclude that the present technology on the high power diode lasers has to be improved by a factor of 10 to 100 to achieve at least more than 10 mJ of 2.1 μm laser output energy from diode-laser-pumped holmium lasers.

Authors would like to acknowledge the technical support provided by Addison T. Inge, Edward A. Modlin and Donald J. Cettemy throughout this research.

References

1. J. T. Lin, "Progress Report: Diode Pumping and Frequency Conversion," Lasers & Optronics, 8(7), 61(1989).
2. G. Kintz, L. Esterowitz, and R. Allen, "Cascade Laser Emission at 2.31 and 2.08 μm from Laser-Diode Pumped Tm, Ho:$LiYF_4$ at Room Temperature," in *Digest of Topical Meeting on Tunable Solid State Lasers* (Optical Society of America, Washington, D.C., 1987), paper MC2-1.
3. G. J. Kintz, L. Esterowitz, and R. Allen, "CW Diode-Pumped Tm^{3+}, Ho^{3+}:YAG 2.1 μm Room-Temperature Laser," Electronics Lett., 23, 616 (1987).
4. T. Y. Fan, G. Huber, R. L. Byer, and P. Mitzscherlich, "Continuous-wave Operation at 2.1 μm of a Diode-Laser-Pumped, Tm-Sensitized Ho:$Y_3Al_5O_{12}$ Laser at 300 K," Opt. Lett., 12, 678 (1987).
5. H. Hemmati, "Diode Laser-Pumped Ho:YLF Laser," in *Digest of Conference on Lasers and Electro-Optics* (Optical Society of America, Washington, D.C., 1987), paper W14.
6. R. Allen, L. Esterowitz, L. Goldberg, J. F. Weller, and M. Storm, "Diode-Pumped 2 μm Holmium Laser," Electronics Lett. 22, 947 (1986)
7. H. Hemmati, "2.07-μm cw diode-laser-pumped Tm,Ho:$YLiF_4$ room-temperature laser," Opt. Lett., 14, 435 (1989).
8. J. Drube, G. Huber, and D. Mateika, "Flashlamp-pumped Cr^{3+}:GSAG and Cr^{3+}:GSGG : Slope Efficiency, Resonator Design, Color Centers and Tunability," in *Tunable Solid-State Lasers II,* A.B. Budgor, L. Esterowitz, and L. C. DeShazer, eds. (Springer-Verlag, New York, 1986), pp. 118-125.
9. J. V. Meier, N. P. Barnes, D. K. Remelius, and M. R. Kokta, "Flashlamp-Pumped Cr^{3+}:GSAG Laser," IEEE J. Quantum Electron., QE-22, 2058 (1986).
10. G. J. Kintz, R. Allen, and L. Esterowitz, "Two for One Photon Conversion Observed in Alexandrite Pumped Tm^{3+},Ho^{3+}:YAG at Room Temperature," in *Digest of Conference on Lasers and Electro-Optics* (Optical Society of America, Washington, D.C., 1987), post-deadline paper ThU4.

11. G. Huber, E. W. Duczynski, and K. Petermann, "Laser Pumping of Ho-, Tm-, Er-Doped Garnet Lasers at Room Temperature," IEEE J. Quantum Electron., QE-24, 920 (1988).

12. J M. Fukumoto, and S. J. Brosnan, "Q-switched operation of a continuous-wave pumped Tm,Ho:YAG laser at 300 K," in *Digest of Conference on Lasers and Electro-Optics* (Optical Society of America, Washington, D.C., 1989), paper TUE4.

13. K. H. Kim, Y. S. Choi, N. P. Barnes, R. V. Hess, C. H. Bair, and P. Brockman, Bull. Am. Phys. Soc. 34, 1685 (1989) paper I4 6.

Figure Captions

Figure 1. Schematic diagram for experimental setup. T: transmission, R: reflectivity, HT: highly transmitive, HR: highly reflective, PR: partially reflective, r: radius of curvature, f: focal length.

Figure 2. Flashlamp-pumped Cr:GSAG laser output energies as a function of the electrical input energy (about 50 shots for each run).

Figure 3. Cr:GSAG laser wavelengths compared to the absorption spectrum of the Ho:Tm:Cr:YAG crystal.

Figure 4. The 2.1 μm holmium laser output energies as a function of the absorbed Cr:GSAG laser energy at mirror reflectivities of 98 % and 95 %.

Figure 5. (a)Top trace: flashlamp pulse (200 μs/div.), Middle trace: Cr:GSAG laser pulse (20 μs/div.), Bottom: holmium laser pulse (5 μs/div.), (b)Details of the Cr:GSAG laser pulse beginning, (c)Details of the holmium laser pulse beginning.

Figure 6. Pulse widths and delay times of the 2.1 μm laser apperance with respect to the Cr:GSAG pump laser pulse biginning as a function of the absorbed Cr:GSAG laser energy for two output mirror reflectivities.

Figure 7. The quasi-cw 2.1 μm holmium laser output powers as a function of the Cr:GSAG pump laser power.

Figure 8. Comparison of the Q-switched output of the 2.1 μm holmium laser with the normal-mode output measured with a mechanical chopper and a 95% reflective output mirror.

Figure 9. (a)Top trace: flashlamp signal, Middle trace: Cr:GSAG pump laser signal, and Bottom trace: Q-switch opening time, 200 μs/div. (b) Pulse shape of typical Q-switched single spike, 1 μs/div.

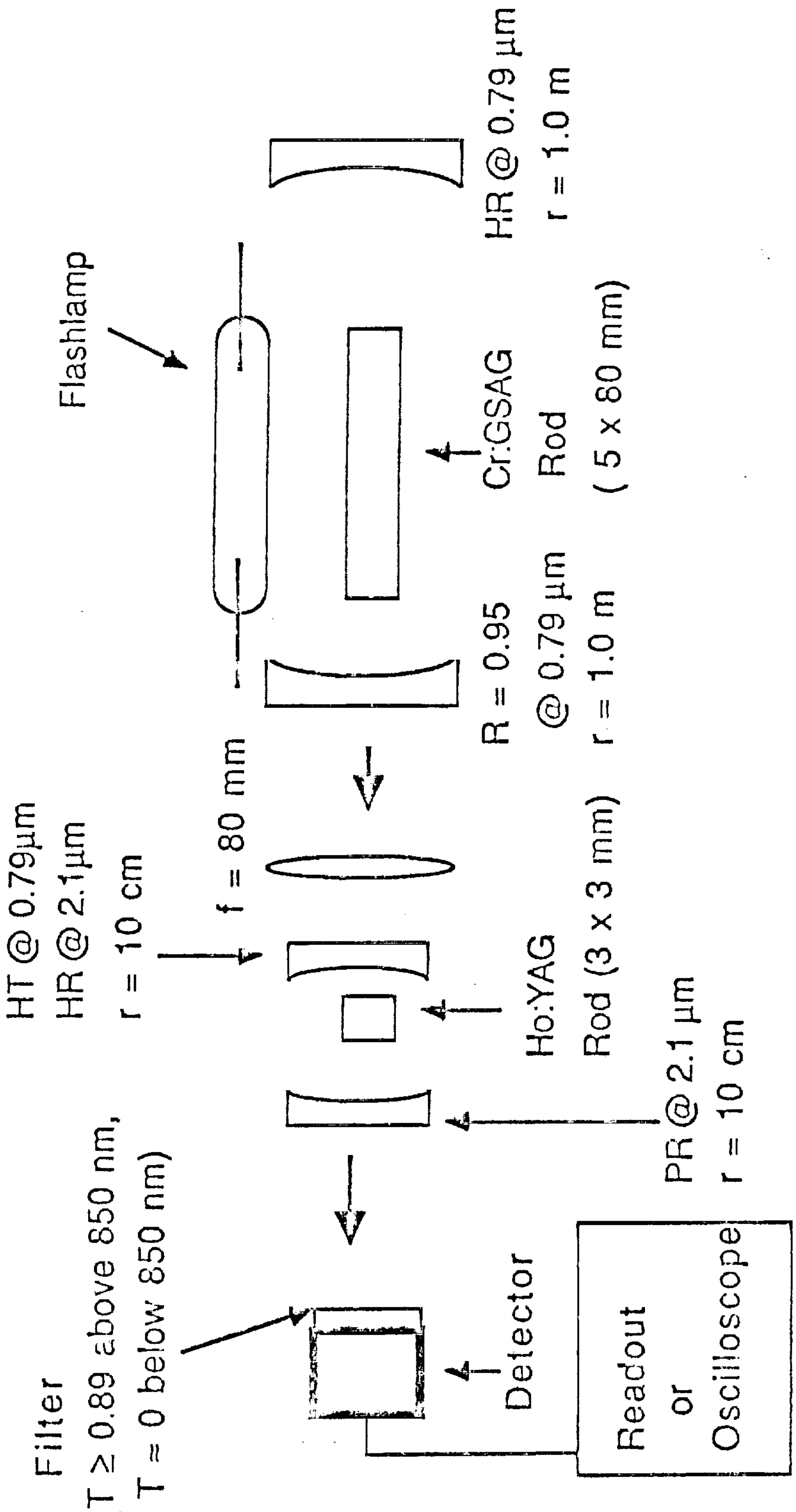

Flashlamp
HR @ 0.79 µm
r = 1.0 m
Cr:GSAG
Rod
(5 x 80 mm)
R = 0.95
@ 0.79 µm
r = 1.0 m
f = 80 mm
HT @ 0.79µm
HR @ 2.1µm
r = 10 cm
Ho:YAG
Rod (3 x 3 mm)
PR @ 2.1 µm
r = 10 cm
Filter
(T ≥ 0.89 above 850 nm,
T = 0 below 850 nm)
Detector
Readout
or
Oscilloscope

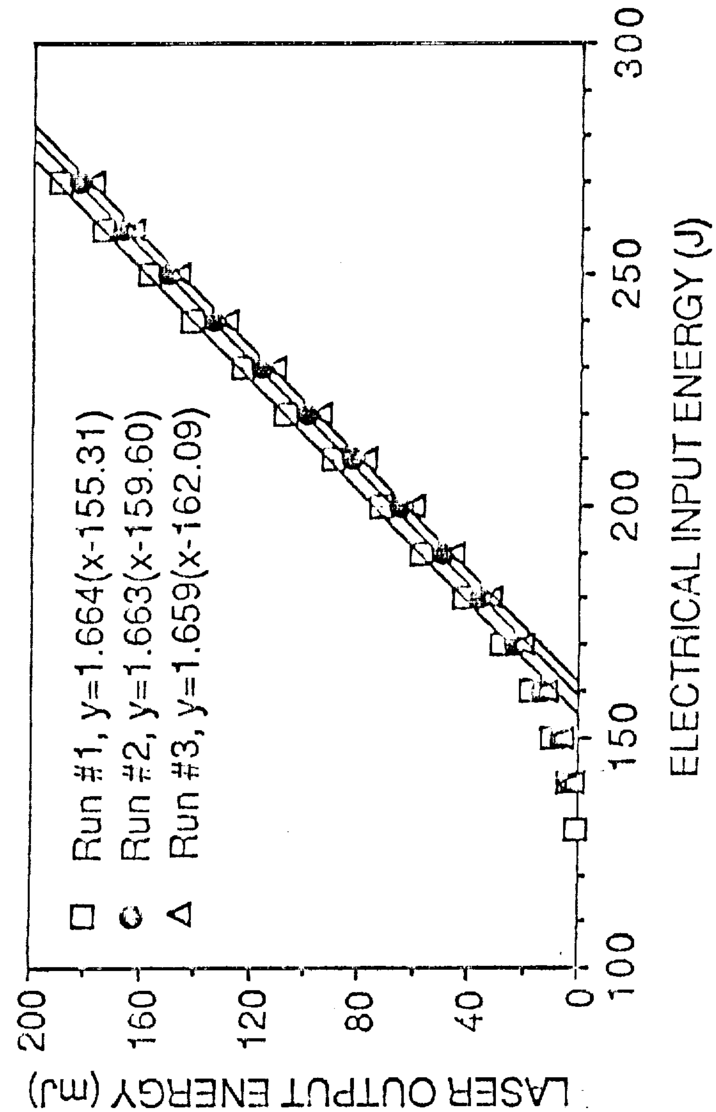

Run #1, y=1.664(x-155.31)
Run #2, y=1.663(x-159.60)
Run #3, y=1.659(x-162.09)
LASER OUTPUT ENERGY (mJ)
ELECTRICAL INPUT ENERGY (J)
0
40
80
120
160
200
100
150
200
250
300

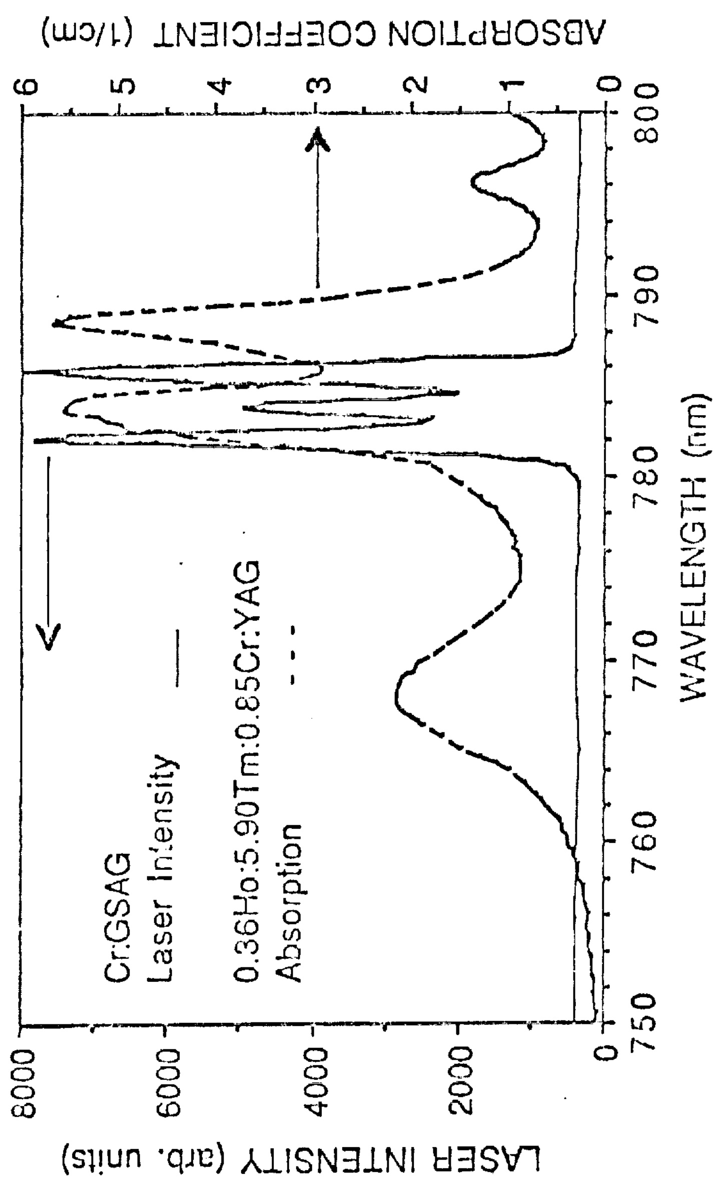
ABSORPTION COEFFICIENT (1/cm)
LASER INTENSITY (arb. units)
WAVELENGTH (nm)
Cr:GSAG
Laser Intensity
0.36Ho:5.90Tm:0.85Cr:YAG
Absorption
0
2000
4000
6000
8000
0
1
2
3
4
5
6
750
760
770
780
790
800

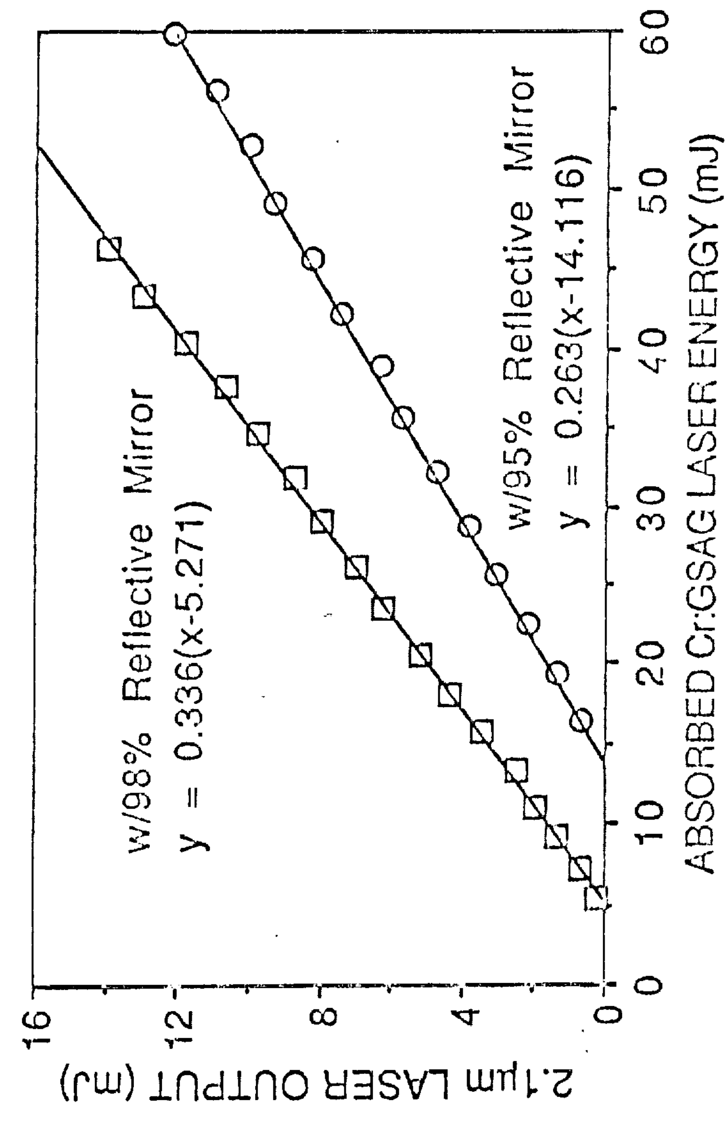
w/98% Reflective Mirror
y = 0.336(x-5.271)
w/95% Reflective Mirror
y = 0.263(x-14.116)
ABSORBED Cr:GSAG LASER ENERGY (mJ)
2.1μm LASER OUTPUT (mJ)
0
10
20
30
40
50
60
0
4
8
12
16

(a)

(b)

(c)

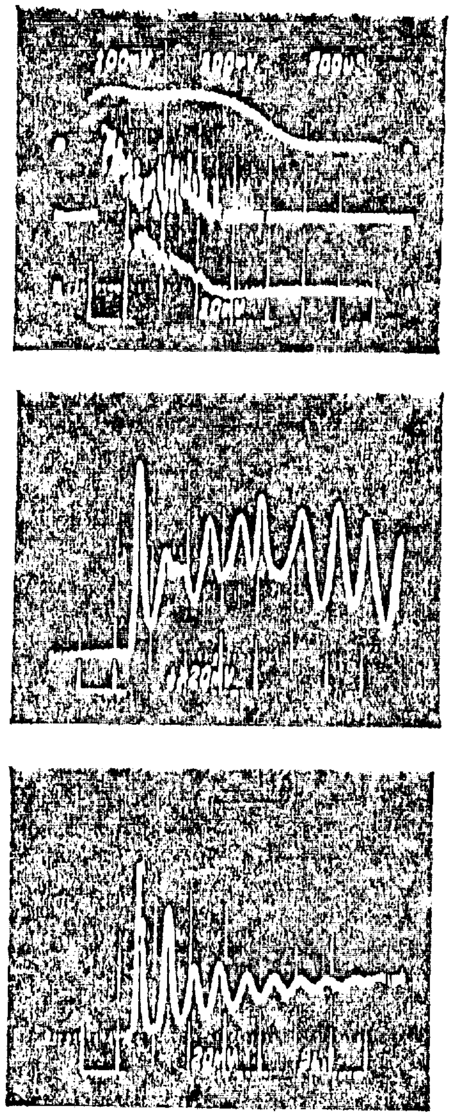

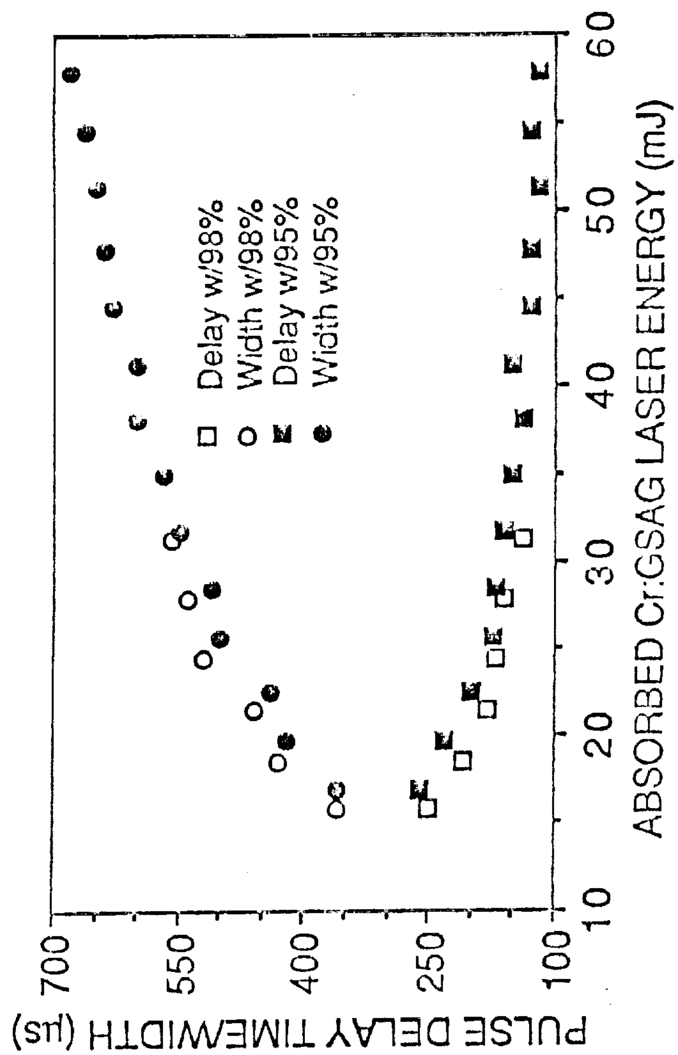
PULSE DELAY TIME/WIDTH (μs)
700
550
400
250
100
10
20
30
40
50
60
ABSORBED Cr:GSAG LASER ENERGY (mJ)
Delay w/98%
Width w/98%
Delay w/95%
Width w/95%

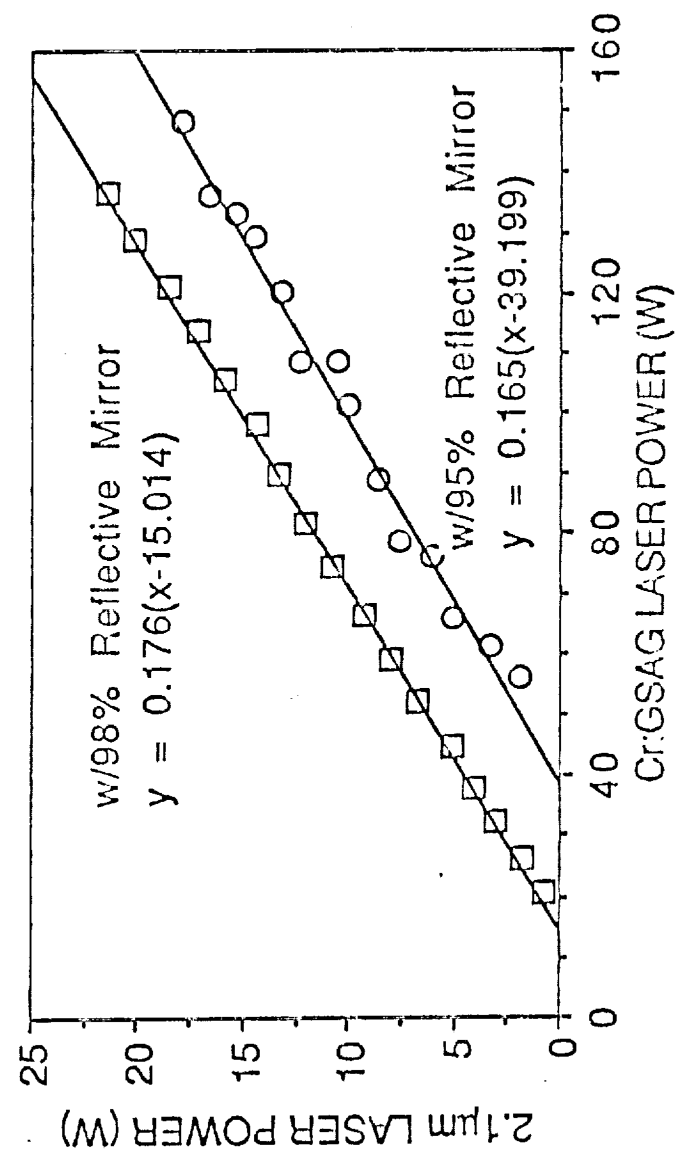
w/98% Reflective Mirror
y = 0.176(x-15.014)
w/95% Reflective Mirror
y = 0.165(x-39.199)
2.1μm LASER POWER (W)
Cr:GSAG LASER POWER (W)
0
5
10
15
20
25
0
40
80
120
160

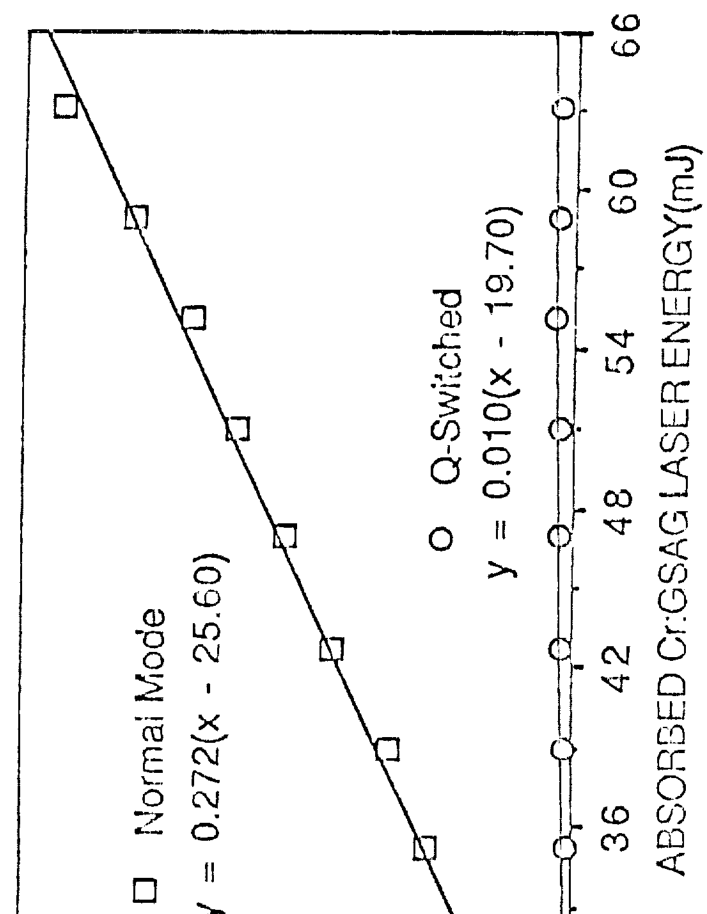

2.1 μm LASER OUTPUT (mJ)
0
3
6
9
12
30
36
42
48
54
60
66
ABSORBED Cr:GSAG LASER ENERGY(mJ)
□ Normal Mode
y = 0.272(x - 25.60)
○ Q-Switched
y = 0.010(x - 19.70)

ORIGINAL PAGE IS
OF POOR QUALITY

(a)

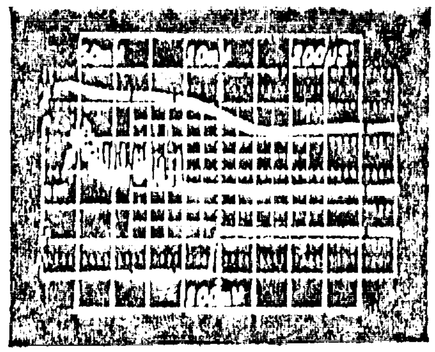

(b)

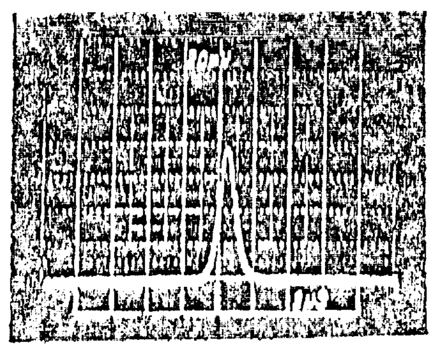

Evaluation of 2.1 μm Ho:Tm:Cr:YAG Lasers Under Flashlamp Pumping at Various Operating Temperatures

Kyong H. Kim, Young S. Choi,
Department of Physics, Hampton University, Hampton, Virginia 23668
and
Norman P. Barnes, Robert V. Hess, Clayton H. Bair, and Philip Brockman
NASA Langley Research Center, Hampton, Virginia 23665

ABSTRACT

Ho:Tm:Cr:YAG crystals with various Tm^{3+} concentrations have been evaluated for flashlamp-pumped normal mode and Q-switched 2.1 μm laser operations under a wide variety of experimental conditions in order to understand internal dynamic processes among the ions and to determine an optimum lasing condition. Laser output parameters, such as energy, slope efficiency, thresholds, pulse length and wavelength, were determined as a function of operating temperature, Tm^{3+} concentration, output mirror reflectivity, input electrical energy and Q-switch opening time. The increase of the laser slope efficiency was observed with the increase of the Tm^{3+} concentration from 2.5 atomic % to 4.5 atomic %. Two laser transitions at 2.098 and 2.091 μm were observed and the possible origin of the 2.091 μm laser transition was identified in this measurement. Q-switched laser output energies corresponding to about 100 % of the normal-mode laser energies were obtained in a strong single spike of pulse length of around 200 ns by optimizing the opening time of a lithium niobate Q-switch. The Q-switch opening time is affected by the energy transfer from Cr^{3+} to Tm^{3+}-ions and from Tm^{3+} to Ho^{3+}-ions and the upper laser level lifetime of the Ho^{3+}-ions.

INTRODUCTION

Development of solid state lasers with Ho^{3+}, Tm^{3+} and(or) Er^{3+} doped crystals have been pursued by NASA for eye-safe mid-infrared LIDAR, light detection and ranging, applications. As a part of the project we have been working on evaluation of Ho^{3+}:Tm^{3+}:Cr^{3+}:YAG crystals for normal-mode and Q-switched 2.1 μm laser operation. Optimum Tm^{3+} concentration in the crystal was sought under flashlamp pumping.

Lasing properties of the Ho^{3+} ion in the mid-infrared region have been studied by many research groups since early 1960's.[1-5] However, the technology of those lasers is still premature for the lidar application. In order to overcome the inefficiency related to narrow absorption bands of the Ho^{3+}, Tm^{3+} and Er^{3+}-ions, Cr^{3+} has been utilized. Improvement of flashlamp-pumped Ho^{3+} laser efficiency has been demonstrated recently by several research groups[6,7] by utilizing the broad absorption spectrum of Cr^{3+} over the flashlamp's emission spectrum and efficient energy transfer to the Tm^{3+} and then to Ho^{3+}-ions. It is known that high Tm^{3+}concentration and low Ho^{3+} concentration are preferred to achieve a quantum efficiency approaching 2 and to avoid large reabsorption losses.[6] However, determination of the optimum Tm^{3+} concentration required to ensure efficient energy transfer from Cr^{3+} to Tm^{3+} and from Tm^{3+} to Ho^{3+} in the Ho:Tm:Cr:YAG crystal has not been made. This paper will present the results obtained with three Ho:Tm:Cr:YAG crystals with 3 different Tm^{3+} concentrations but similar Cr^{3+} and Ho^{3+} concentrations.

QUANTUM PROCESSES in Ho^{3+}, Tm^{3+} and Cr^{3+}-IONS

The energy levels of the Cr^{3+}, Tm^{3+} and Ho^{3+}-ions and the energy transfer mechanisms among those ions in a YAG crystal are illustrated in Fig.1. The use of Cr^{3+} for flashlamp pumping is based on its broad absorption spectrum provided by the transitions from the ground $^4A_2$ state to the upper $^4T_1$ and $^4T_2$ states and Subsequent near resonant efficient energy transfer from the Cr^{3+} to the $^3H_4$ state of the Tm^{3+}-ions. Fig.2 shows the absorption spectrum of the Ho^{3+}(0.45 atomic %):Tm^{3+}(2.5 at. %):Cr^{3+}(1.5 at. %):YAG crystal. Two broad bands in the visible region correspond to the chromium absorption. Other sharp peaks correspond to the absorption by the holmium and thulium ions.

For high Tm concentrations, the transition from the $^3H_4$ manifold to the $^3F_4$ manifold induces the cross relaxation process which provides two Tm ions in the $^3F_4$ manifolds from a single Tm ion in the $^3H_4$ manifold. As a result, the quantum efficiency approaches two. Then, the near resonant energy transfer process from the $^3F_4$ Tm manifold to the $^5I_7$ Ho manifold provides efficient pumping mechanism of the Ho-ions. Buoncristiani, et al's work showed that the energy transfer processes between Cr^{3+} and Tm^{3+} between Tm^{3+} and Ho^{3+} as well as the cross-relaxation process are more effective in crystals with high Tm^{3+} concentrations[8].

In order to operate the 2.1 μm Ho laser efficiently at room temperature, the Ho^{3+} concentration must be low. The increase of the Ho^{3+} concentration increases the ground state population of the Ho^{3+} $^5I_8$ level which causes high resonant reabsorption losses for the $^5I_7$(Ho)- $^5I_8$(Ho) laser transition. However, as the temperature goes down, the upper levels of the lower laser manifold ($^5I_8$) of the Ho^{3+}-ion becomes thermally unpopulated and the efficiency of the laser performance increases. Since the upper laser level lifetime of the Ho^{3+}-ion is longer than 5 ms even at room temperature, an efficient storage time for the Q-switch operation is possible. Contrary to the normal-mode operation a high Ho^{3+} concentration may be effective for a high Q-switched laser output because the high Ho^{3+} concentration can provide more ions in the upper laser levels.

EXPERIMENTAL METHODS

The experimental configuration used in this research is shown in Fig.3. The temperature of the laser rod was varied from 120 K to room temperature by circulating liquid nitrogen vapor around the rod. The flashlamp was cooled by circulating deionized water. The flashlamp and laser rod were placed in an aluminum pumping cavity of a shape of 76.2 mm long cylindrical ellipse with major and minor axes of 152.4 mm and 149.1 mm respectively. The detailed cavity design was reported elsewhere.[9] In order to achieve thermal isolation, the entire pumping cavity was placed in an vacuum system. Cood thermal isolation was necessary since the cooling capacity of liquid nitrogen vapor was limited. A 450 torr Xe flashlamp with 4 mm bore diameter and 76.2 mm arc length was used and surrounded by a uranium doped flow tube water jacket to reduce possible solarization effects. The size of the Ho:Tm:Cr:YAG laser rod used was 4 mm in diameter and 55 mm in length.

Since the Ho:Tm:Cr:YAG has a long upper laser level lifetime, the pulse forming network (PFN) for the flashlamp was designed for long pulse operations. With a 146.5 μF capacitor and a 184 μH inductor critically damped pulses of 350 μs FWHM pulse length were obtained at an input voltage of 905 volts, which corresponds to the electrical input energy of 60 J. A highly reflective mirror at 2.1 μm with a 10 m radius curvature is attached to the one end of the vacuum box as a window, and an antireflection coated quartz flat was placed on the other side of the vacuum box. Flat mirrors with various reflectivities were used as output couplers. The total resonator length was 88 cm. In Q-switched operations a lithium niobate crystal, $LiNbO_3$, of dimensions of 9 mm x 9 mm x 25 mm was used as a Q-switch. A ZnSe plate of 2.17 mm thickness was used to polarize the laser beam at Brewster angle. The hold-off voltage for the Q-switch crystal was 1.62 kV. The Q-switch trigger signal could be delayed from 0 to several ms with respect to the trigger for the flashlamp.

The laser output energy and pulse shape were measured with a pyroelectic energy meter and with a liquid N_2 cooled HgCdTe detector, respectively. The temporal responsibility of the HgCdTe detector and an accompanying preamplifier was better than 10 MHz. For the wavelength measurement the Ho:Tm:Cr:YAG laser beam was sent to a spectrometer through a folding mirror which was a highly reflective mirror at 2.1 μm and detected by a thermo-electrically cooled InAs detector.

RESULTS

Fig.4 shows the typical normal-mode laser output energies of the Ho(0.45 %):Tm(3.5 %):Cr(1.5 %):YAG crystal measured as a function of the electrical energy stored in capacitor with various output mirrors at an operating temperature of 140 K. As expected, the slope efficiency and threshold energy increase with the decreasing mirror reflectivity. The measured normal-mode laser output energies of the Ho(0.45 %):Tm(2.5 %):Cr(1.5 %):YAG crystal as a function of operating temperature at various electrical input energies with a 60 % reflectivity mirror are shown in Fig. 5. The decrease of the laser output energy with the increasing temperature clearly indicates the effect due to thermal population in the lower laser level. Fig. 6(a) shows the comparative plot of the laser slope efficiency of the two laser rods of 2.5 % and 3.5 % Tm^{3+} concentrations as function of the operating temperature with various output mirrors while Fig. 6(b) shows the comparative plot of the laser slope efficiency of the three laser rods of 2.5, 3.5 % and 4.5 % Tm^{3+} concentrations as function of the operating temperature with a 98 % reflective output mirror. Since our system was not optimized for a high efficiency, the slope efficiencies are not comparable to other's but still provide good comparative results on the effect of the different Tm^{3+} concentration. The decrease of the slope efficiency with increase of the operating temperature can be explained with the decrease of the transfer efficiency of the Cr^{3+} to Tm^{3+} and Tm^{3+} to Ho^{3+} which is observed in spectroscopic measurement. Fig. 7 shows the measured fluorescence from the Ho:Tm(2.5 at %):Cr:YAG crystal as a function of temperature. As the crystal temperature increases, the 2.1 μm fluorescence coming mainly from the Ho^{3+} ions decreases while the 1.7 μm fluorescence coming from the Tm^{3+} ions increases. This is an evidence of lowering the Tm^{3+} to Ho^{3+} transfer with the increase of t can be seen in the 2.1 and 1.7 μm fluorescence measurements. The increase of the slope efficiency with the increase of the Tm^{3+} concentration from 2.5 to 4.5 at % is related to the increase of the transfer processes among the Cr^{3+}, Tm^{3+} and Ho^{3+} as well as the increase of the cross-relaxation within Tm^{3+}. A detailed spectroscopic study on the dependence of these transfer and cross-relaxation processes upon temperature and Tm^{3+} concentration can be found in Ref. 8. On the other hand, the increase of the threshold with the increase of the operating temperature as shown in Fig. 8 can be explained with the increase of the lower laser level population.

The measured low slope efficiency may be attributed to the relatively small crystal diameter compared to the mode diameter, about 2.8 mm, and poor optical coupling between the flashlamp and the laser rod. The poor coupling is due to the short laser rod compared with the length of the flashlamp and the low cavity reflectivity which was less than 80 % at 633 nm.

The measured Q-switched and normal-mode laser output ratio is plotted in Fig.9 at various input energies and temperatures as a function of the $LiNBO_3$ electro-optic Q-switched delay time with respect to the beginning of the flashlamp pulse. The output mirror used in this comparative measurement had a 60 % reflectivity and the normal-mode operation was done with the Q-switch crystal and ZnSe polarizer in the resonator. The Q-switched laser outputs equal to or slightly higher than the normal mode outputs were achieved in the form of a strong single spike by optimizing the Q-switched opening times at the given input energies and temperatures. The pulse length of the single spike is ranged from 150 to 300 ns depending on the output energy. As expected, the pulse length becomes narrow with the increasing output energy. Thus, the obtainable Q-switched laser efficiency can be as the same as the normal-mode laser efficiency. However, the Q-switched laser measurements made in this research were limited at the output energies below 25 mJ to avoid optical damage on the crystals.

During the normal-mode operation multiple spikes corresponding to relaxation oscillation were observed and the interval between the spikes was measured to be about 15 μs. On the other hand, several irregular spikes, considerably fewer than in normal-mode case, were observed with the Q-switch opening before and near the end of the pump pulse as also observed by Storm[10], while a strong single spike was observed at relatively late Q-switch opening times which correspond delay times of longer than 1 ms from the beginning of the 350 μs (FWHM) long flashlamp light. The intensities of each of the multiple Q-switched spikes are much stronger than those of the normal-mode spikes, and the their total energy was finally appeared with the strong single spike at the delayed Q-switch openings. The multiple Q-switched spikes were possibly caused by Boltzmann energy redistribution within the Tm $^3F_4$ and Ho $^5I_7$ states and slow energy transfer processes from Cr^{3+} to Tm^{3+} and from Tm^{3+} to Ho^{3+}. Especially the long delay time required for the strong single spike attributes to the relatively long transfer time for the Cr^{3+} to Tm^{3+} transfer rather than the Tm^{3+} to Ho^{3+} transfer process since the Cr^{3+} to Tm^{3+} transfer time is expected to be about of the order of 1 ms for the given concentrations according to Buoncristiani, et al.'s work[8] while the Tm^{3+} to Ho^{3+} transfer time is shorter than 50 μs.

Laser wavelengths measured at various conditions are shown in Figs. 10 through 12. Fig. 10(a) shows the laser wavelengths measured at various operating temperatures with the 0.45%Ho: 3.5%Tm: 1.5%Cr:YAG crystal, output mirror reflectivity of 60 % and input electrical energy of 60 J. At low temperatures two laser transitions at 2.098 and 2.091 μm were observed, but the 2.098 μm line is stronger than the 2.091 μm line while the 2.091 μm line becomes dominant at high temperatures. Fig. 10(b) shows the results of the same measurement as Fig. 10(a) except the output mirror's reflectivity of 98 %. For the highly reflective output mirror the 2.098 μm line is dominant over all temperatures. The detailed line structures should not be paid too much attention because the spectra was obtained by scanning over many consecutive shots and the flashlamp-pumped laser system is not uniform over many shots.

Figs. 11(a) and (b) show the laser wavelengths measured near threshold at various temperatures with 60 % and 98 % reflective output mirrors, respectively. For the low reflective output mirror the transition of the laser wavelength from 2.098 to 2.091 μm is seen apparently with increasing the temperature while the two laser lines coexist at high temperatures for the high reflective output mirror. These results can be explained by calculating the threshold values of the two laser lines. Fan, et al.'s paper shows that the stimulated emission cross section of the 2.091 μm line is higher than that of the 2.098 μm at room temperature.[11] This means that, in a high loss resonator with low pump power, the line with high stimulated emission cross section can build up quickly compared to any other lines. Fig. 12 shows the detailed energy level diagram of the $^5I_7$ and $^5I_8$ manifolds of the Ho^{3+} and possible laser transitions. The level energy values indicated on the left were the ones obtained by Ashurov, et al. at 4.2 °K.[12] So far there has been several different laser transitions observed near 2.1 μm from the Ho^{3+} doped YAG laser crystals by others in many different operating conditions.[11, 13-15] However, only two laser lines with relatively large stimulated emission cross sections compared to other lines were observed in our measurement. There has been no report published so far, as far as we know, to identify the 2.091 μm laser line. Based on the calculation on the given energy level values several transitions are possible for the 2.091 μm line, but our results on the laser wavelength measurement indicate that the 2.091 μm laser transition originates from high lying manifolds of the $^5I_7$ state because the 2.091 μm line is dominant at high temperatures. Thus, the solid lines on the Fig. 12 indicate the possible transitions for the two laser lines. No significant change of the laser lines was observed when the input energy was varied to 60 J and when the Q-switched operation was compared to the normal-mode operation.

CONCLUSION

Ho:Tm:Cr:YAG crystals with 3 different Tm^{3+} concentrations have been studied for both normal-mode and Q-switched 2.1 μm laser operation as well as fluorescence measurement under flashlamp pumping at various operating temperatures, various output mirror reflectivities, various input energies and various Q-switch opening times. The effect of temperature and Tm^{3+} concentration on the laser performance was investigated, and the improvement of the laser efficiency was observed with the increase of the Tm^{3+} concentration from 2.5 to 4.5 atomic %. Q-switched laser efficiencies close to the normal-mode efficiencies were obtained with optimum Q-switch conditions. Laser line transitions were also examined at various conditions and the origin of the 2.091 μm laser line was well understood.

ACKNOWLEDGEMENT

Authors acknowledge that Mark E. Storm and Coherent Technology provided the laser crystals and Edward A. Modlin, Lewis G. Burnie, Donald J. Cettemy, Addison T. Inge and Keith E. Murray provided the technical support during the course of this research work. Authors also appreciate valuable discussion with Dr. A. Martin Buoncristiani.

REFERENCES

1. L. F. Johnson, G. D. Boyd, K. Nassau, Proc. IRE., **50**, 87 (1962).
2. E.P. Chicklis, C. S. Naiman, R. C. Folweileer, D. R. Gabbe, H. P. Jenssen, and A. Linz, Appl. Phys. Lett. **19**, 119 (1971).
3. N. P. Barnes and D. J. Gettemy, IEEE J. Quantum Electron., **QE-17**, 1303 (1981).
4. H. Lotem, Y. Kalisky, J. Kagan, and D. Sagie, IEEE J. Quantum Electron., 24, 119 (1988).
5. E. W. Duczynski and G. Huber, Appl. Phys. Lett., 48, 1562 (1986).
6. P. Mitzscherlich, in Tunable Solid-State Lasers II (Edited by Budgor, *et al.*), Springer-Verlag, New York, (1986) p. 282.
7. I. A. Shcherbakov, in Tunable Solid-State Lasers II (Edited by Budgor, *et al.*), Springer-Verlag, New York, (1986) p. 293.
8. A. M. Buoncristiani, G. Armagan, B.Di Bartolo, and J. J. Swetits, in Proceedings of the Ninth Course; "Advances in Nonradiative Processes in Solids," held in Erice, Italy, June 15 - 29 (1989).
9. D. Gettemy, N. P. Barnes, and E. Griggs, **51**, 1194 (1980).
10. M. Storm, Appl. Opt. **27**, 4170 (1988).
11. T. Y. Fan, G. Huber, R. L. Byer, and P. Mitzscherlich, IEEE J. Quantum Electron., QE-24, 924 (1988).
12. M. Kh. Ashurov, Yu. K. Voron'ko, E. V. Zharikov, A. A. Kaminskii, V. V. Osiko, A. A. Solo', M. I. Timoshechkin, V. A. Fedorov, and A. A. Shabaltai, Izvestiya Akademii Nauk SSSR, Neorganicheskie Materialy, **15**, 1250 (1979).
13. L. F. Johnson, J. E. Geusic, and L. G. Van Uitert, Appl. Phys. Lett. **7**, 127 (1965).
14. L. F. Johnson, J. E. Geusic, and L. G. Van Uitert, Appl. Phys. Lett. 8, 200 (1966).
15. D. P. Devor, and B. H. Soffer, IEEE J. Quantum Electron. **QE-3**, 231 (1972).

FIGURE CAPTIONS

Fig. 1 Energy transfer processes in a Ho:Tm:Cr:YAG crystal.

Fig. 2 Absorption spectrum of a Ho:Tm:Cr:YAG crystal of concentration of 0.45 atomic % Ho^{3+}, 2.5 at % Tm^{3+} and 1.5 at % Cr^{3+}.

Fig. 3 Schematic diagram for experimental setup.

Fig. 4 Normal-mode laser output energy of the 0.45 at %Ho:3.5 %Tm:1.5 at % Cr:YAG crystal as a function of electrical input energy at 140 K.

Fig. 5 Normal-mode laser output energy of the 0.45 at % Ho:2.5 % Tm:1.5 at % Cr:YAG crystal measured with a 60 % reflective output mirror as a function of the operating temperature.

Fig. 6 (a) Slope efficiency of the 2.1 μm Ho:Tm:Cr:YAG lasers with Tm^{3+} concentrations of 2.5 and 3.5 atomic % measured with various output mirrors as a function of temperature. (b) Slope efficiency of the 2.1 μm Ho:Tm:Cr:YAG lasers with Tm^{3+} concentrations of 2.5, 3.5 and 4.5 atomic % measured with a 80 % reflective output mirror as a function of temperature.

Fig. 7 2.1 and 1.7 μm fluorescence measured from a flashlamp-pumped 0.45 at % Ho:2.5 at % Tm:1.5 at % Cr:YAG crystal as a function of temperature at a fixed input energy of 60 J.

Fig. 8 Threshold input electrical energy of the 0.45 at % Ho:2.5 at % Tm:1.5 at % Cr:YAG laser as a function of the operating temperature measured with various output mirrors.

Fig. 9 Ratio of the normal-mode and Q-switched laser output energies of the 0.45 at % Ho:3.5 at % Tm:1.5 at % Cr:YAG laser as a function of the Q-switch opening delay time.

Fig. 10 (a) The normal-mode laser wavelengths of the 0.45 at % Ho:3.5 at % Tm:1.5 at % Cr:YAG crystal measured at various operating temperatures with a 60 % reflective output mirror and input electrical energy of 60 J. (b) The same as (a) but with a 98 % reflective mirror.

Fig. 11 (a) The near threshold normal-mode laser wavelengths of the 0.45 at % Ho:3.5 at % Tm:1.5 at % Cr:YAG crystal measured at various operating temperatures with a 60 % reflective output mirror. (b) The same as (a) but with a 98 % reflective mirror.

Fig. 12 Energy level diagram of the Ho^{3+} $^5I_7$ and $^5I_8$ manifolds and the observed laser transitions.

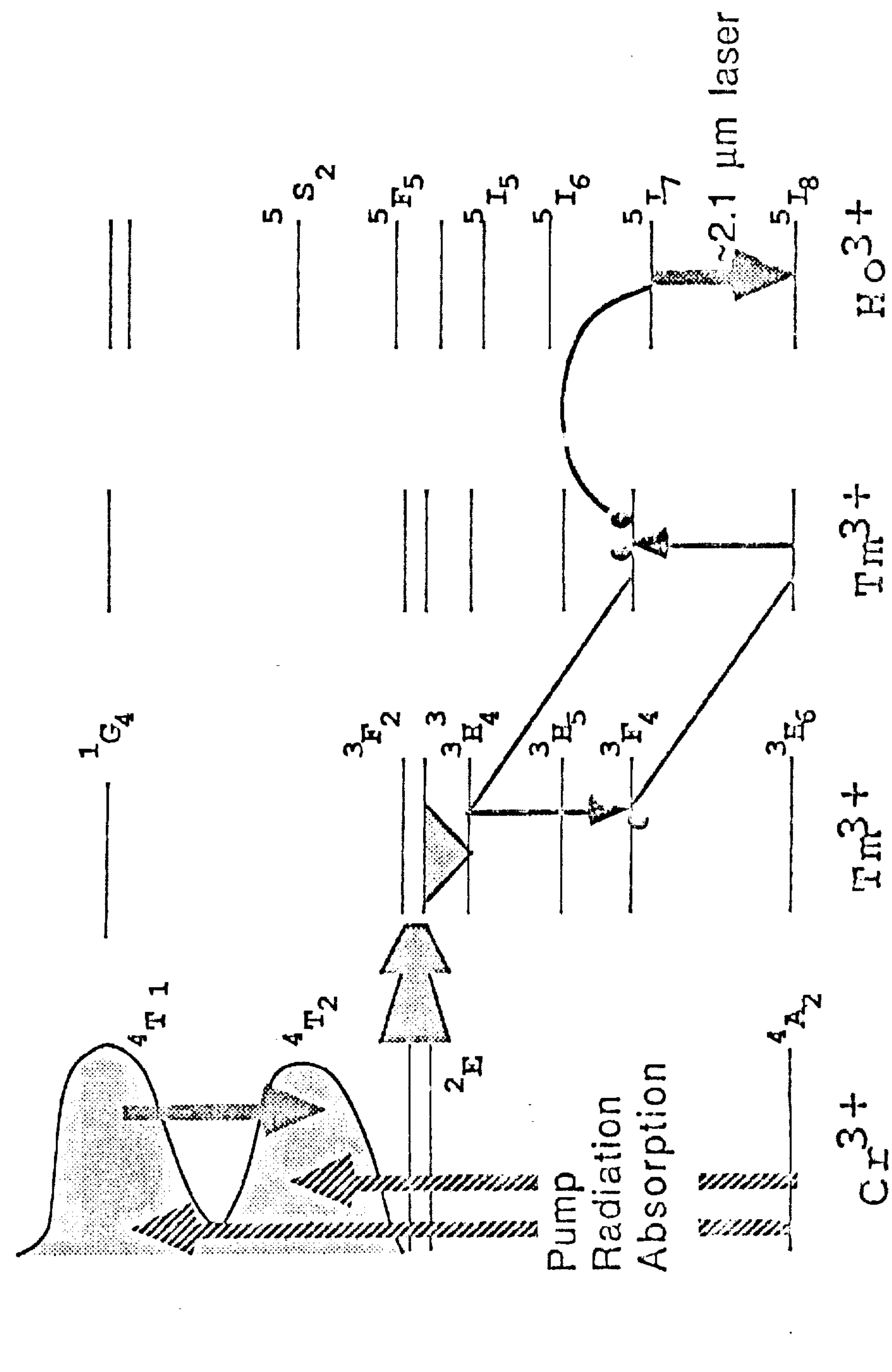

Pump
Radiation
Absorption
Cr^{3+}
$^4T_1$
$^4T_2$
^2E
$^4A_2$
Tm^{3+}
$^1G_4$
$^3F_2$
$^3F_3$
$^3H_4$
$^3H_5$
$^3F_4$
$^3H_6$
Tm^{3+}
Ho^{3+}
$^5S_2$
$^5F_5$
$^5I_5$
$^5I_6$
$^5I_7$
$^5I_8$
~2.1 μm laser

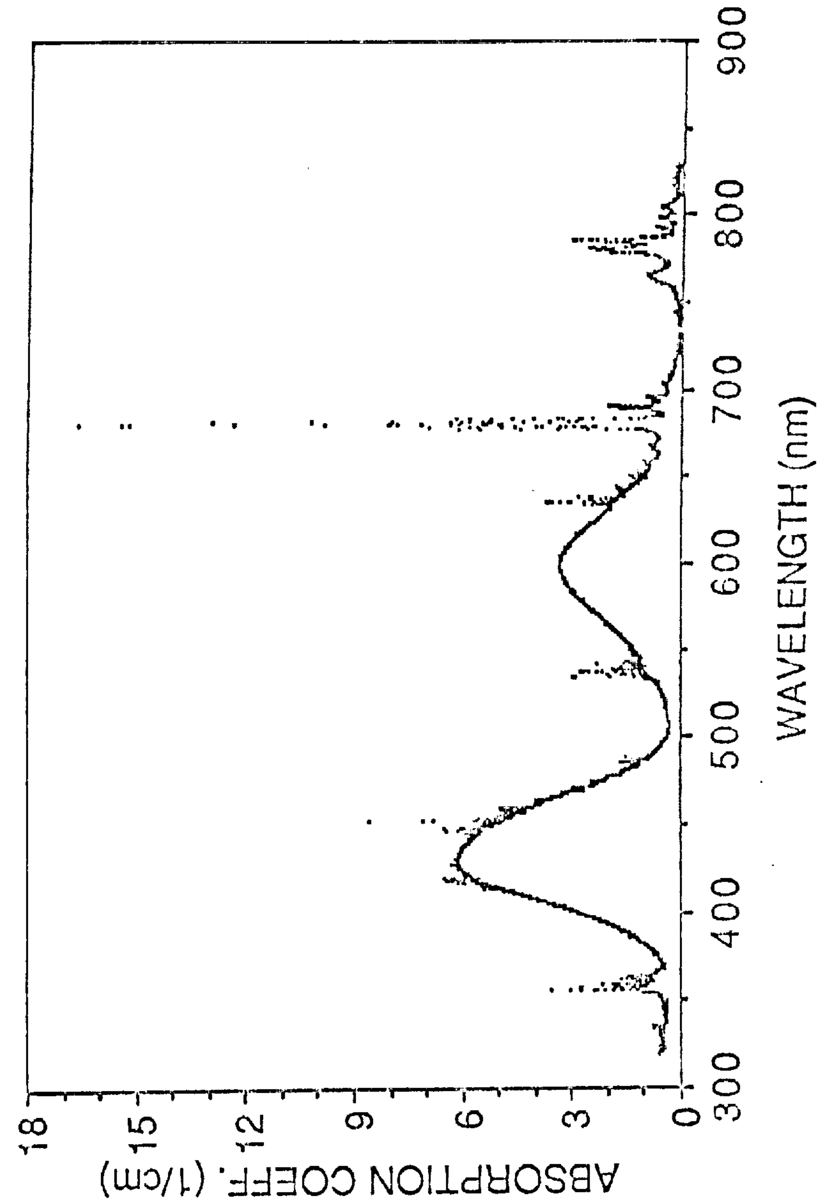
ABSORPTION COEFF. (1/cm)
WAVELENGTH (nm)
0
3
6
9
12
15
18
300
400
500
600
700
800
900

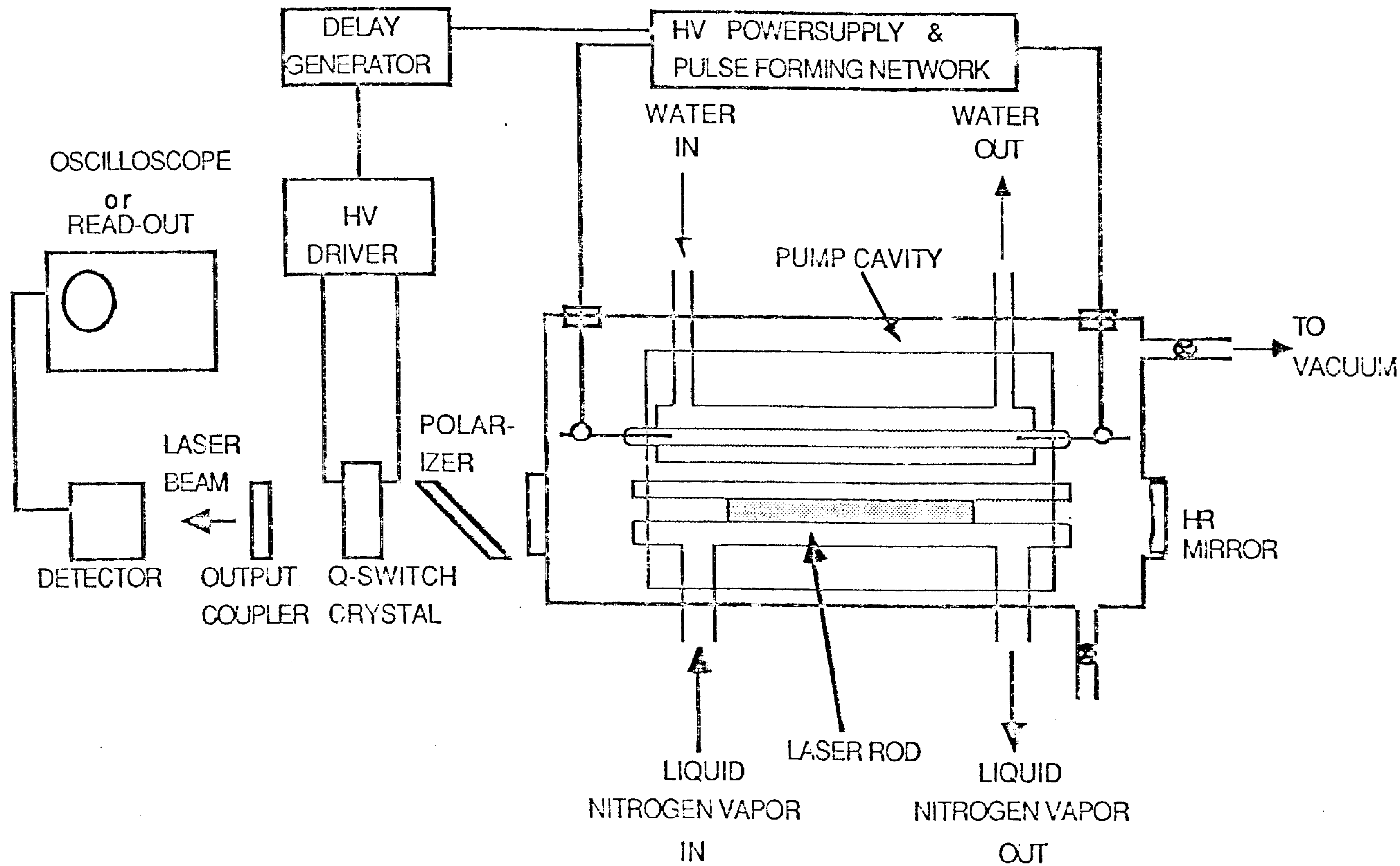
DELAY GENERATOR
HV POWERSUPPLY & PULSE FORMING NETWORK
WATER IN
WATER OUT
OSCILLOSCOPE or READ-OUT
HV DRIVER
PUMP CAVITY
TO VACUUM
POLAR-IZER
LASER BEAM
HR MIRROR
DETECTOR
OUTPUT COUPLER
Q-SWITCH CRYSTAL
LASER ROD
LIQUID NITROGEN VAPOR IN
LIQUID NITROGEN VAPOR OUT

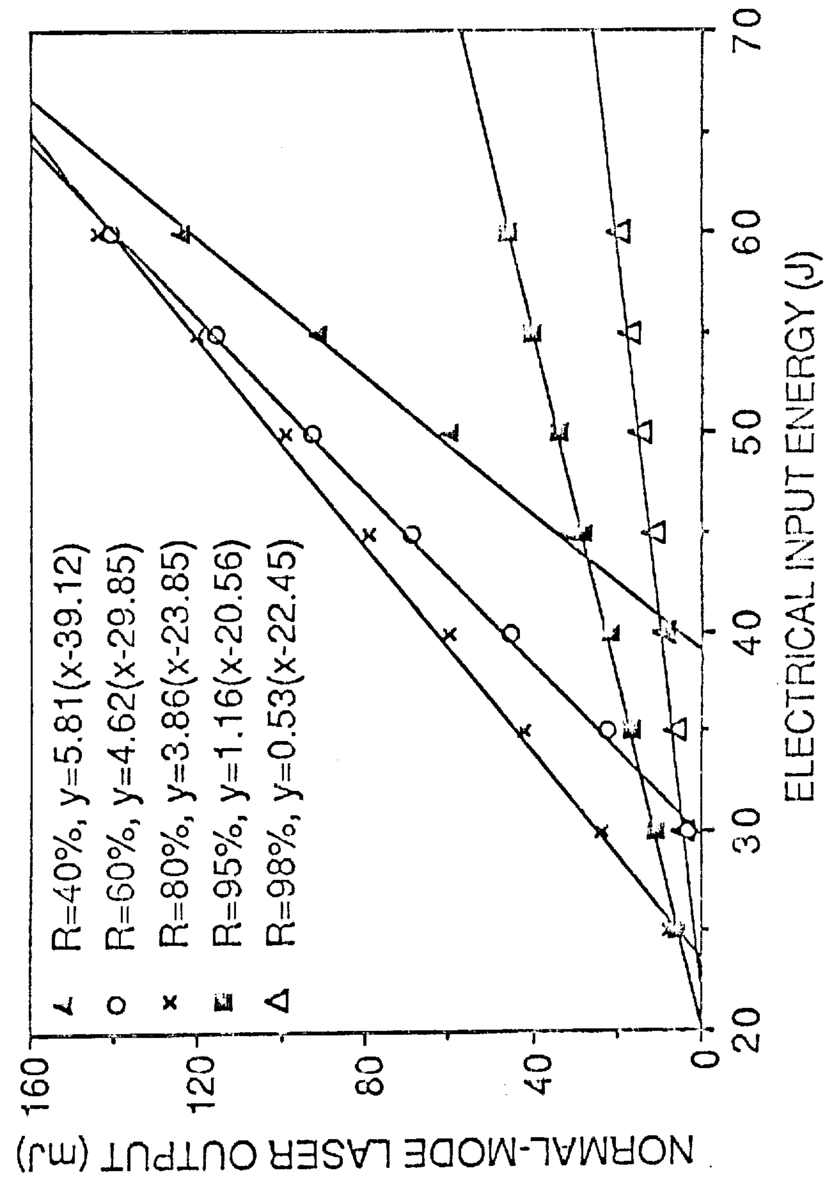
R=40%, y=5.81(x-39.12)
R=60%, y=4.62(x-29.85)
R=80%, y=3.86(x-23.85)
R=95%, y=1.16(x-20.56)
R=98%, y=0.53(x-22.45)
NORMAL-MODE LASER OUTPUT (mJ)
ELECTRICAL INPUT ENERGY (J)
0
40
80
120
160
20
30
40
50
60
70

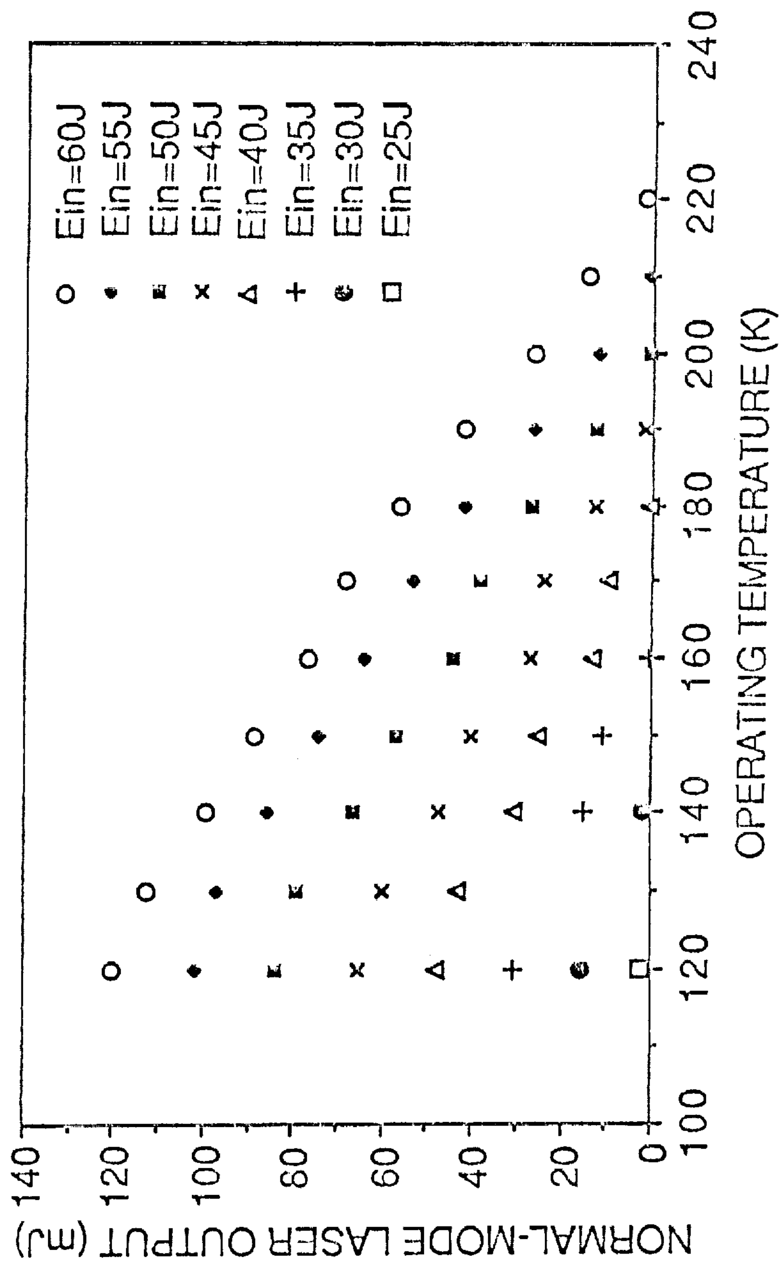
NORMAL-MODE LASER OUTPUT (mJ)
OPERATING TEMPERATURE (K)
Ein=60J
Ein=55J
Ein=50J
Ein=45J
Ein=40J
Ein=35J
Ein=30J
Ein=25J
0
20
40
60
80
100
120
140
100
120
140
160
180
200
220
240

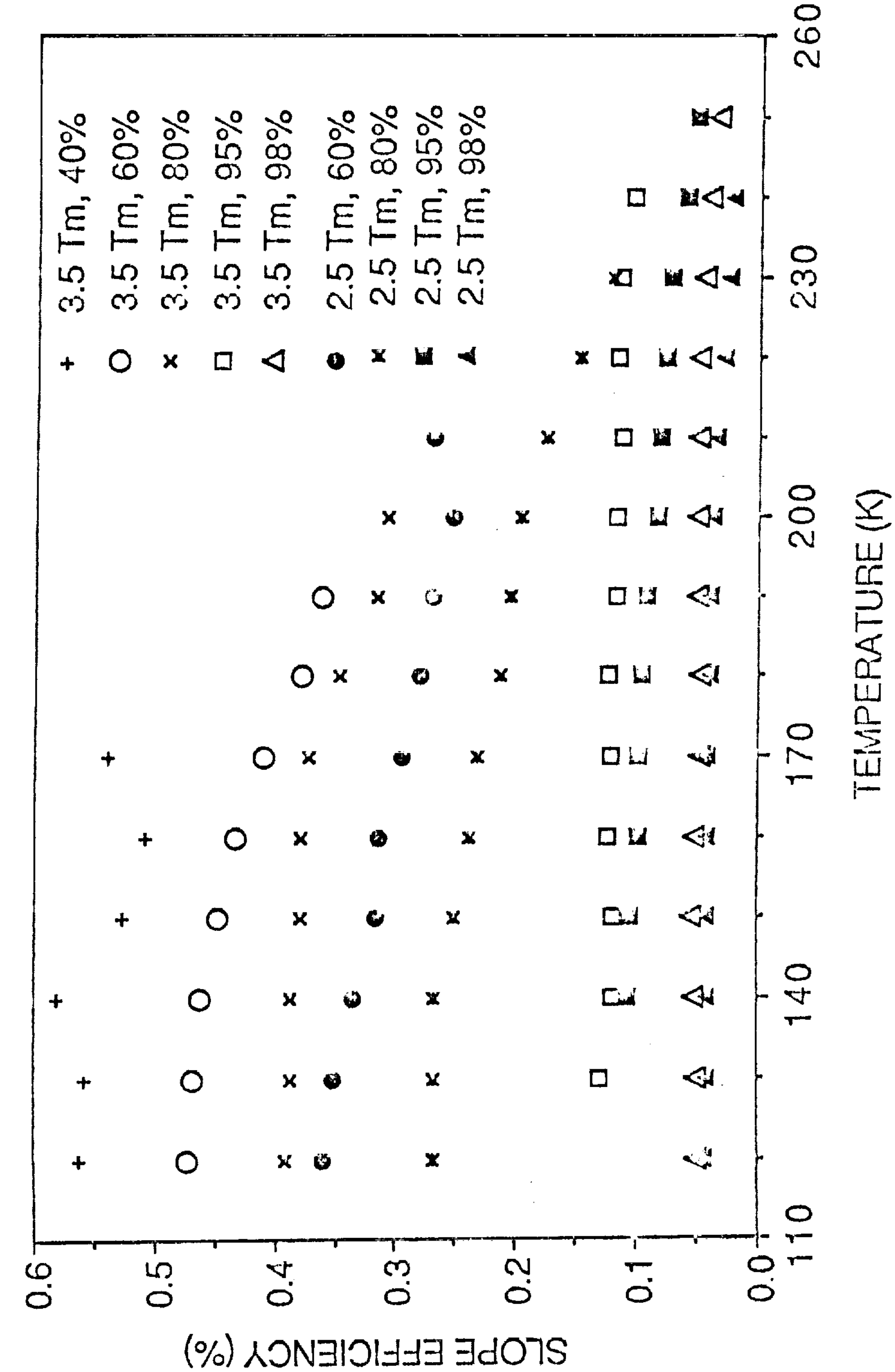

SLOPE EFFICIENCY (%)
TEMPERATURE (K)
0.0
0.1
0.2
0.3
0.4
0.5
0.6
110
140
170
200
230
260
3.5 Tm, 40%
3.5 Tm, 60%
3.5 Tm, 80%
3.5 Tm, 95%
3.5 Tm, 98%
2.5 Tm, 60%
2.5 Tm, 80%
2.5 Tm, 95%
2.5 Tm, 98%

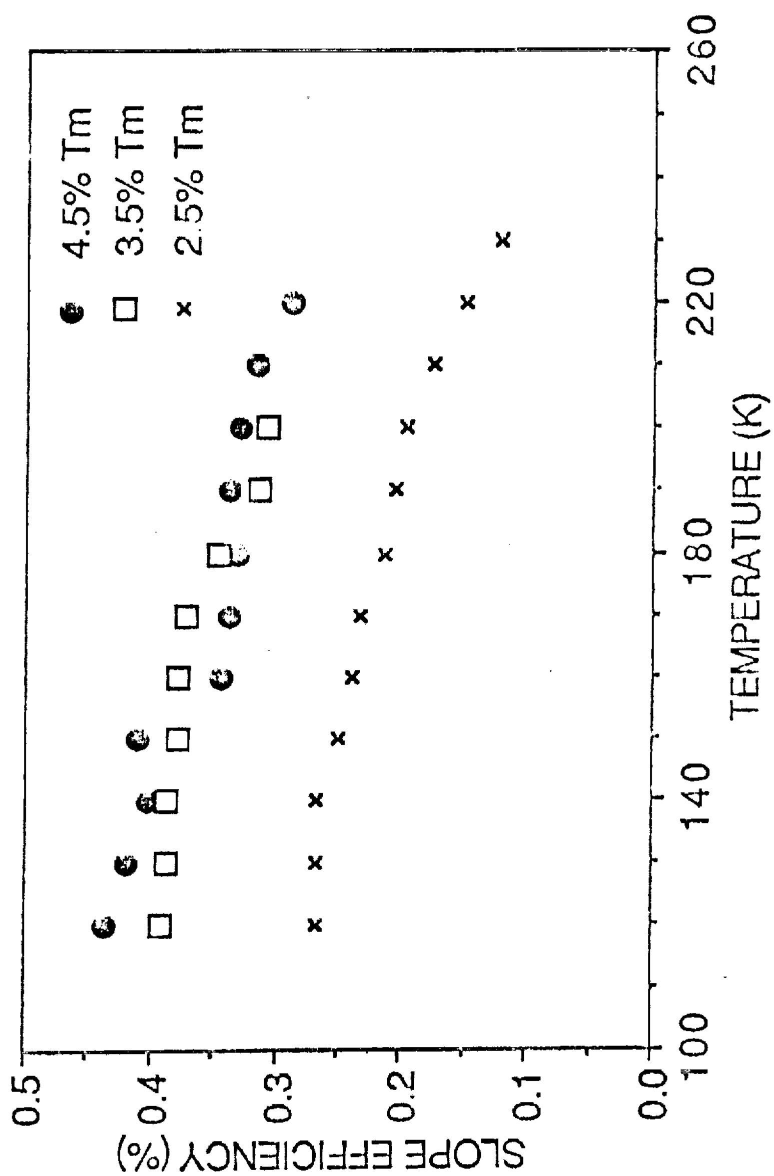
4.5% Tm
3.5% Tm
2.5% Tm
SLOPE EFFICIENCY (%)
0.5
0.4
0.3
0.2
0.1
0.0
TEMPERATURE (K)
100
140
180
220
260

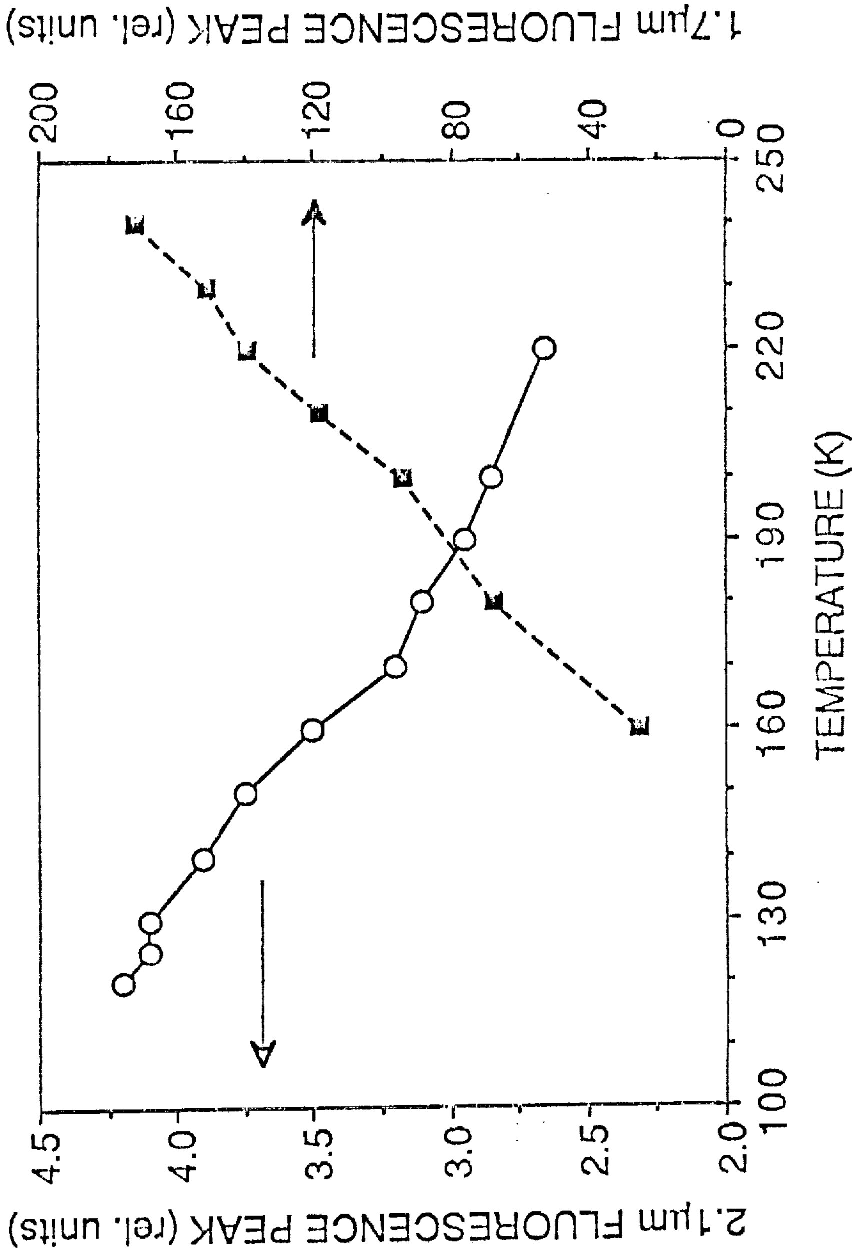
1.7μm FLUORESCENCE PEAK (rel. units)
0
40
80
120
160
200
2.1μm FLUORESCENCE PEAK (rel. units)
2.0
2.5
3.0
3.5
4.0
4.5
TEMPERATURE (K)
100
130
160
190
220
250

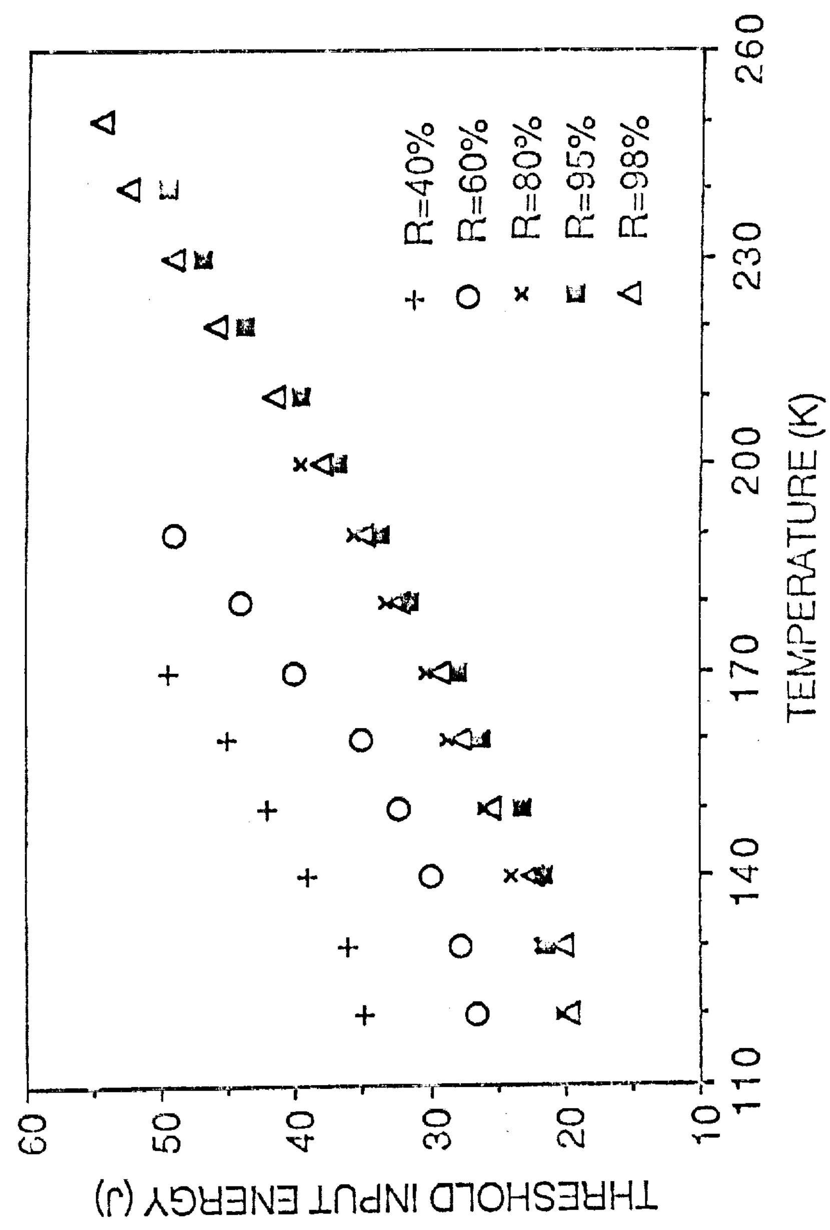

THRESHOLD INPUT ENERGY (J)
TEMPERATURE (K)
10
20
30
40
50
60
110
140
170
200
230
260
+ R=40%
○ R=60%
× R=80%
■ R=95%
△ R=98%

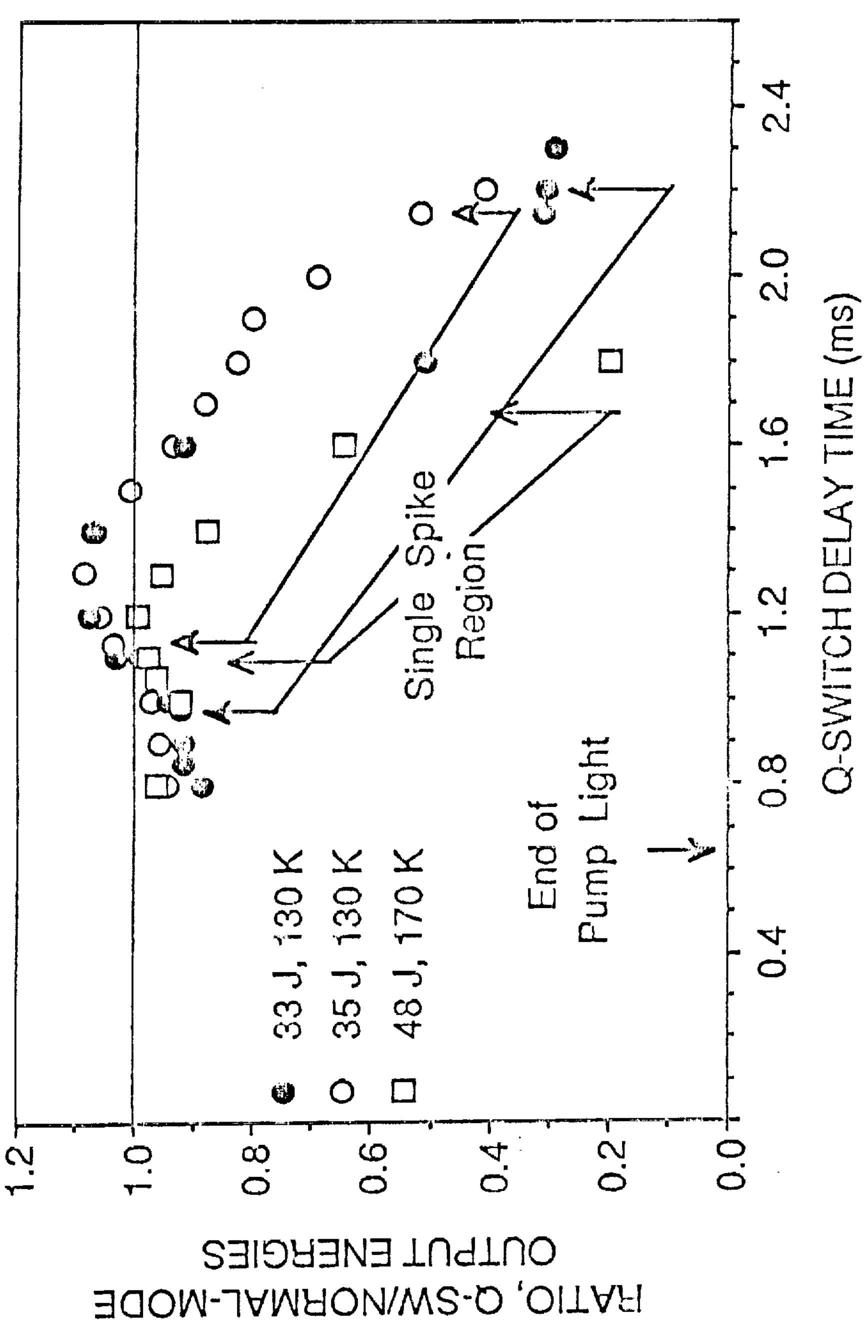
RATIO, Q-SW/NORMAL-MODE OUTPUT ENERGIES
Q-SWITCH DELAY TIME (ms)
33 J, 130 K
35 J, 130 K
48 J, 170 K
End of Pump Light
Single Spike Region
1.2
1.0
0.8
0.6
0.4
0.2
0.0
0.4
0.8
1.2
1.6
2.0
2.4

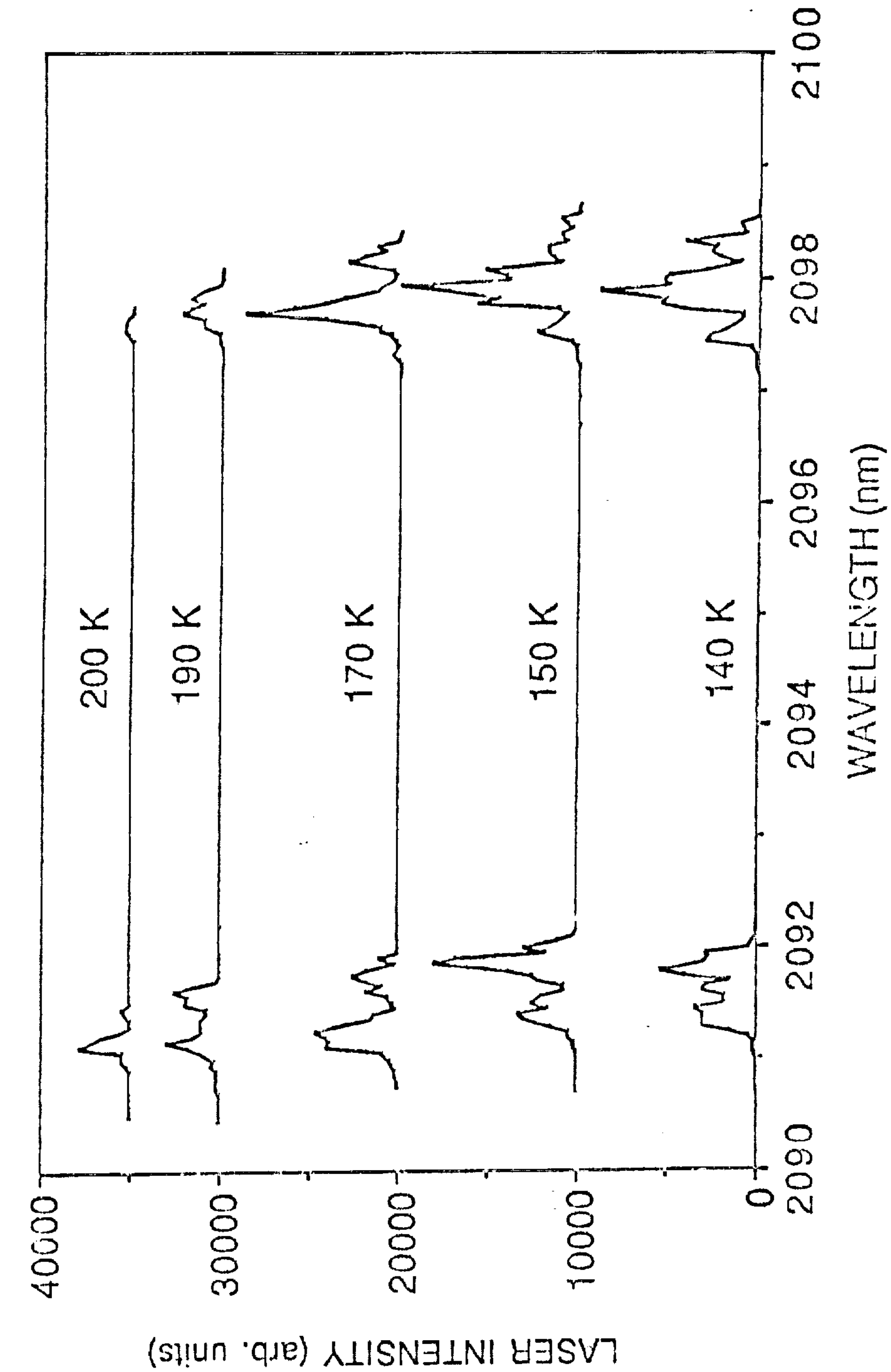

200 K
190 K
170 K
150 K
140 K
2090
2092
2094
2096
2098
2100
WAVELENGTH (nm)
0
10000
20000
30000
40000
LASER INTENSITY (arb. units)

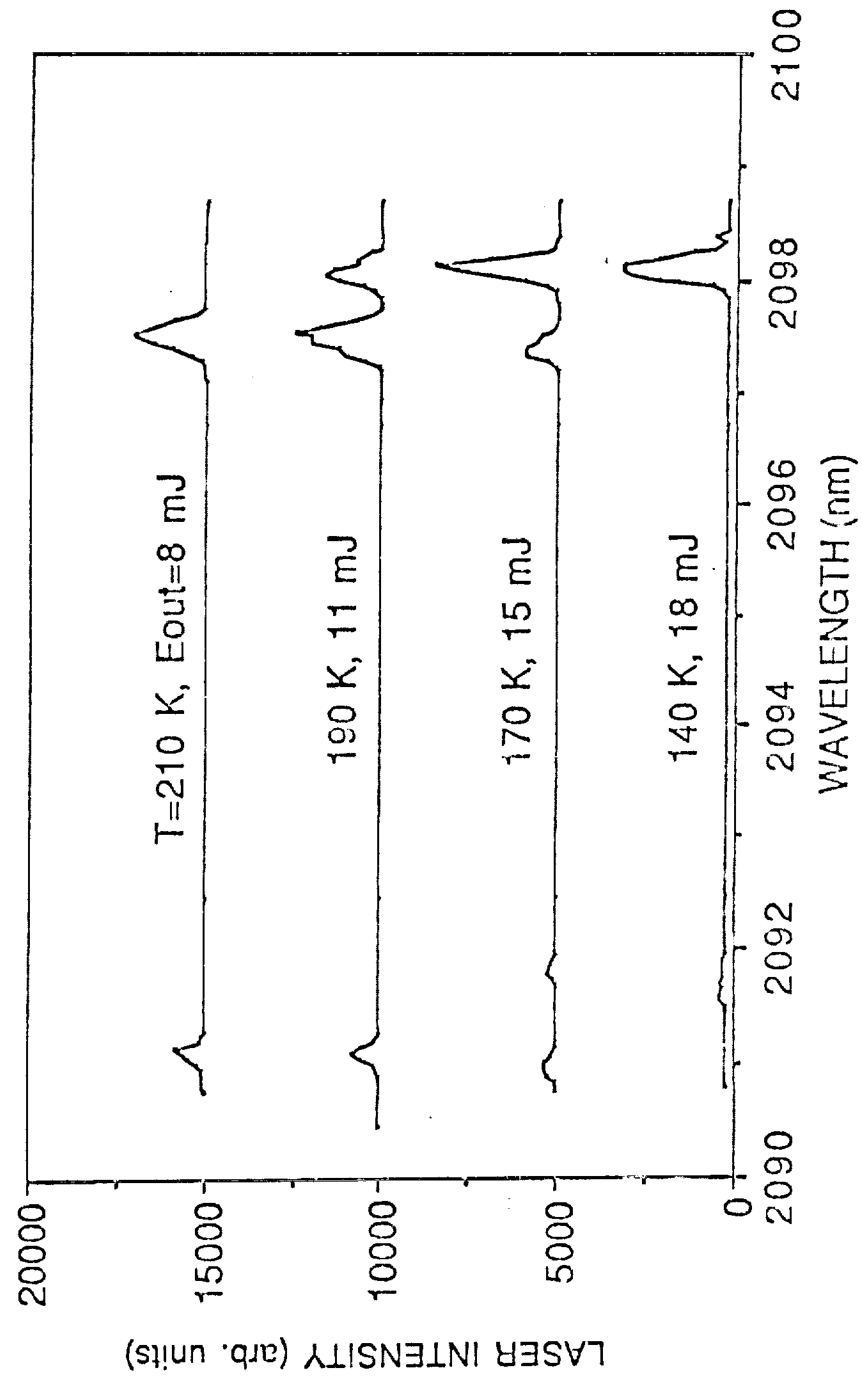
T=210 K, Eout=8 mJ
190 K, 11 mJ
170 K, 15 mJ
140 K, 18 mJ
WAVELENGTH (nm)
2090
2092
2094
2096
2098
2100
LASER INTENSITY (arb. units)
0
5000
10000
15000
20000

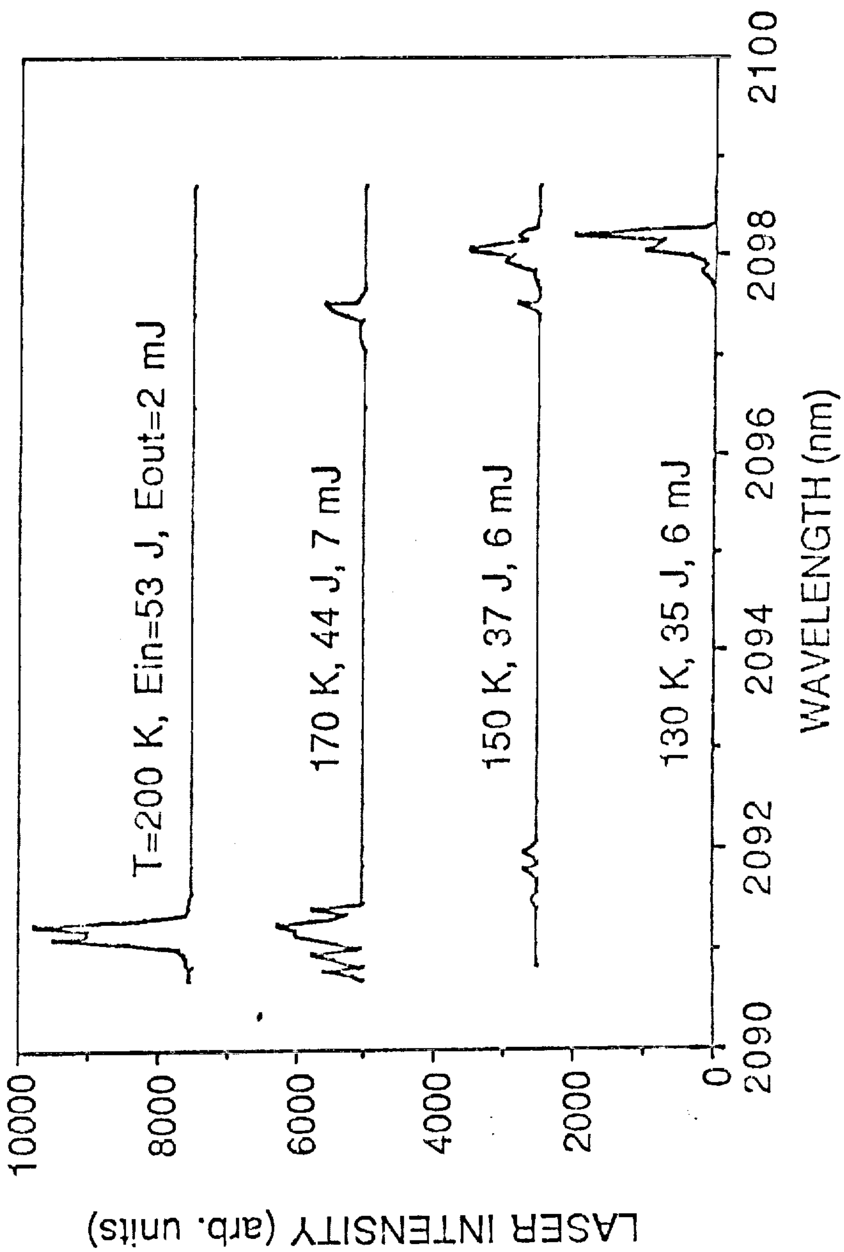
T=200 K, Ein=53 J, Eout=2 mJ
170 K, 44 J, 7 mJ
150 K, 37 J, 6 mJ
130 K, 35 J, 6 mJ
WAVELENGTH (nm)
LASER INTENSITY (arb. units)
2090
2092
2094
2096
2098
2100
0
2000
4000
6000
8000
10000

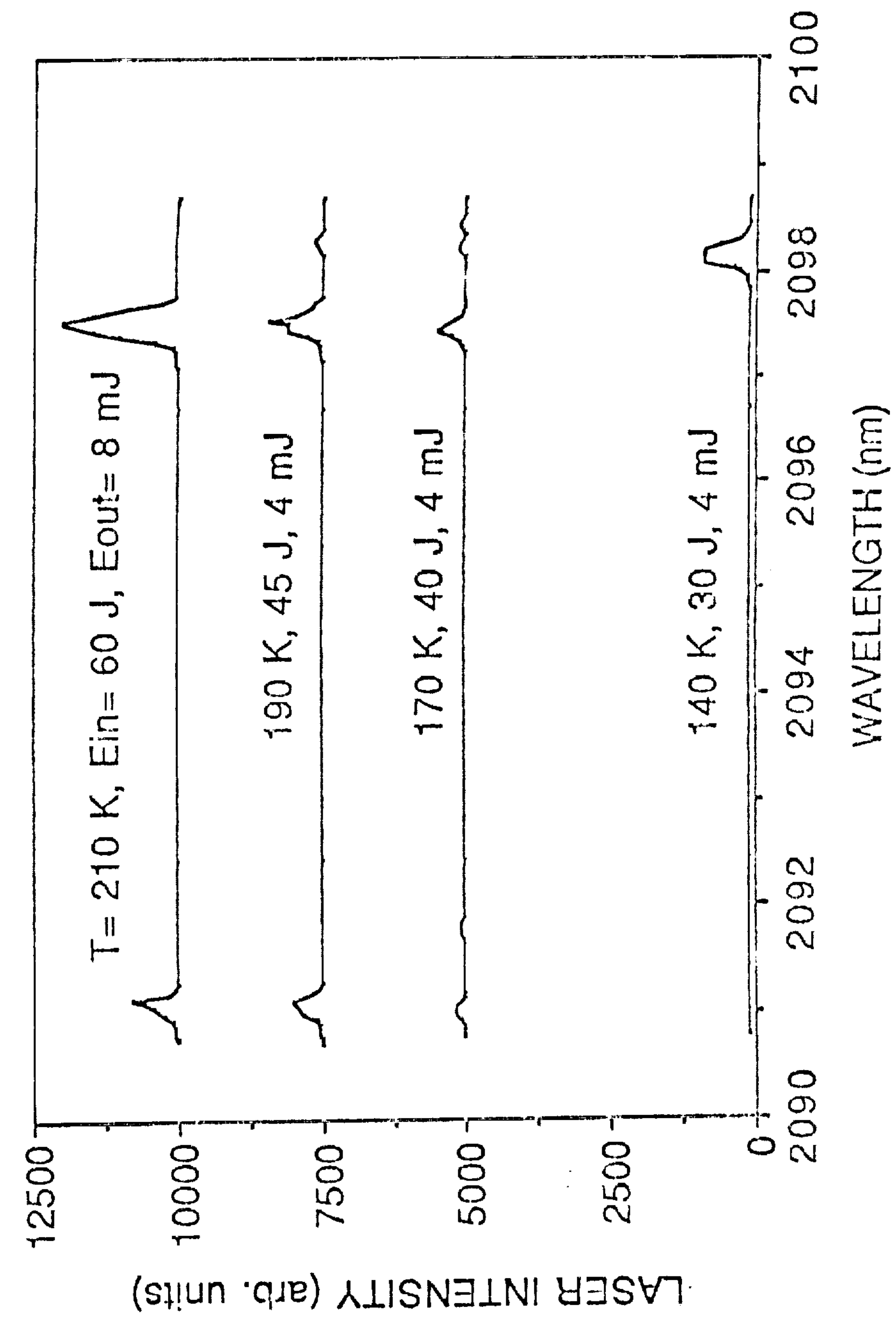
T= 210 K, Ein= 60 J, Eout= 8 mJ
190 K, 45 J, 4 mJ
170 K, 40 J, 4 mJ
140 K, 30 J, 4 mJ
WAVELENGTH (nm)
LASER INTENSITY (arb. units)
2090
2092
2094
2096
2098
2100
0
2500
5000
7500
10000
12500

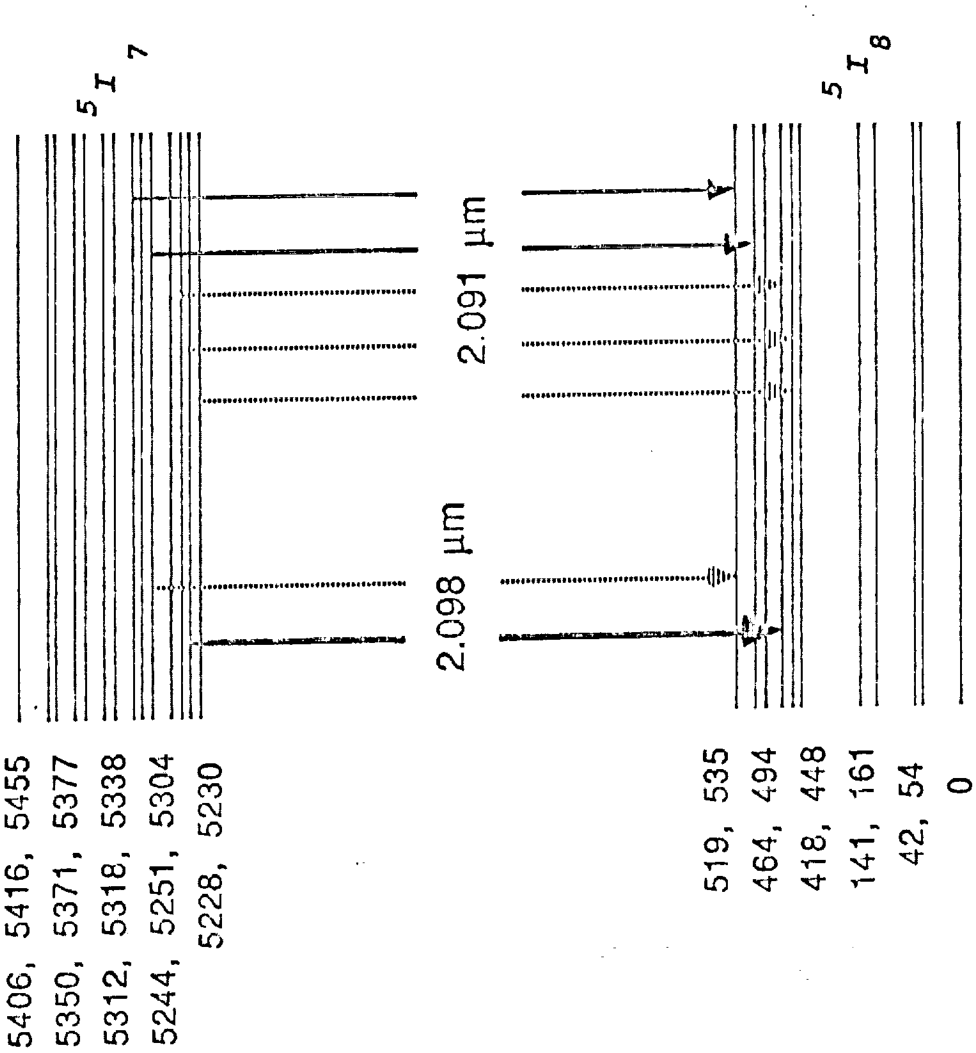

5406, 5416, 5455
5350, 5371, 5377
5312, 5318, 5338
5244, 5251, 5304
5228, 5230
$^5I_7$
2.091 µm
2.098 µm
519, 535
464, 494
418, 448
141, 161
42, 54
0
$^5I_8$